



The author(s) shown below used Federal funding provided by the U.S. Department of Justice to prepare the following resource:

Document Title: Investigations on the Cellular and Morphologic Characteristics of Cranial Vault Fracture: Research and Development of a Time Since Fracture Protocol and Database

Author(s): Carolyn V. Isaac, Ph.D., Jered B. Cornelison, Ph.D., Joseph A. Prahlow, M.D., Clara J. Devota

Document Number: 301143

Date Received: June 2021

Award Number: 2017-DN-BX-0166

This resource has not been published by the U.S. Department of Justice. This resource is being made publically available through the Office of Justice Programs' National Criminal Justice Reference Service.

Opinions or points of view expressed are those of the author(s) and do not necessarily reflect the official position or policies of the U.S. Department of Justice.

National Institute of Justice

FINAL REPORT

Project Number: 2017-DN-BX-0166

***Investigations on the Cellular and Morphologic Characteristics of Cranial Vault Fracture:
Research and Development of a Time Since Fracture Protocol and Database***

Principle Investigators:

Carolyn V. Isaac, Ph.D.
Assistant Professor
517-432-6251
cvisaac@msu.edu

Jered B. Cornelison, Ph.D.
Assistant Professor
269-337-6170
Jered.Cornelison@med.wmich.edu
*Submitting Official

Joseph A. Prahlow, M.D.
Professor
269-337-6164
Joseph.Prahlow@med.wmich.edu

Prepared by: Clara J. Devota, Carolyn V. Isaac, Jered B. Cornelison

Institution:

WMU Homer Stryker M.D. School of Medicine
1000 Oakland Drive
Kalamazoo, MI 49008-5581

Project Period: 01/01/2018 to 12/31/2020

Award Amount: \$576,060

Submitted: 05/26/2021

This project was supported by the National Institute of Justice [award number 2017-DN-BX-0166]. The opinions, findings, and conclusions or recommendations expressed in this publication are those of the authors and do not necessarily reflect those of the U.S. Department of Justice.

TABLE OF CONTENTS

PROJECT SUMMARY	3
PURPOSE	3
MAJOR GOALS AND OBJECTIVES.....	3
RESEARCH GOAL 1: DEVELOP A DATABASE OF CRANIAL FRACTURES OF KNOWN AGE	4
<i>Research Design, Methods, and Analytical and Data Analysis Techniques</i>	4
<i>Expected Applicability of the Research</i>	6
<i>Participants and Other Collaborating Organizations</i>	6
<i>Design Alterations</i>	7
<i>Activities/Accomplishments</i>	8
<i>Results and Findings</i>	11
RESEARCH GOAL 1A: DECALCIFICATION AGENT AND SAMPLE PRESERVATION	12
<i>Research Design, Methods, Analytical and Data Analysis Techniques</i>	12
<i>Expected Applicability of the Research</i>	15
<i>Participants and Other Collaborating Organizations</i>	15
<i>Results and Findings</i>	15
RESEARCH GOAL 2: EVALUATE HISTOLOGICAL ENVIRONMENT OF FRACTURE SAMPLE	19
<i>Research Design, Methods, Analytical and Data Analysis Techniques</i>	19
RESEARCH GOAL 2A: INTEROBSERVER ERROR	22
<i>Research Design, Methods, Analytical and Data Analysis Techniques</i>	22
<i>Expected Applicability of the Research</i>	22
<i>Results and Findings</i>	23
RESEARCH GOAL 2B: STAINING AND CRANIAL HISTOLOGY	25
<i>Research Design, Methods, Analytical and Data Analysis Techniques</i>	25
<i>Expected Applicability of the Research</i>	26
<i>Design Alterations</i>	26
<i>Results and Findings</i>	27
RESEARCH GOAL 2C: FEATURES AND STAGES OF CRANIAL VAULT FRACTURE HEALING	28
<i>Research Design, Methods, Analytical and Data Analysis Techniques</i>	28
<i>Expected Applicability of the Research</i>	31
<i>Participants and Other Collaborating Organizations</i>	31
<i>Results and Findings</i>	31
<i>Infant and Juvenile Healing</i>	37
<i>Stages of Healing in the Adult Cranial Vault</i>	48
DISCUSSION	50
CONCLUSION	51
LIMITATIONS	53
COLLABORATING INSTITUTIONS	55
SCHOLARLY PRODUCTS PRODUCED/IN PROGRESS	56
ACKNOWLEDGEMENTS	58
BIBLIOGRAPHY.....	59
APPENDIX	61

Project Summary

Purpose

Determining the time since injury of skeletal fractures provides forensic practitioners with a means of establishing or corroborating timelines leading up to death, as well as discerning situations of abuse. This is especially true for deaths resulting from trauma to the cranial vault, which can be indicative of both accidental and non-accidental injury. Despite this, the empirical basis from which investigators can accurately and precisely age cranial fractures remains largely unexplored. Conversely, the development of fracture healing models and methods for the estimation of postcranial fracture age are the focus of several scientific inquiries¹⁻⁴; however, these postcranial descriptions of healing and dating methods cannot be applied to cranial fractures due to differences in osseous development⁵ and biomechanical stress between the postcranium and cranium⁶. The current scientific literature shows there are no standards for dating fractures of the cranial vault. The impetus for this research was to remedy the scant understanding of the cellular and tissue responses involved in fracture healing in the human calvarium, providing the foundation for further inquiry into osseous repair in the cranium.

Major Goals and Objectives

The primary goals of this study were threefold, with each phase informing the following. The first was to develop a deidentified online database of cranial injuries of known age with associated decedent information and injury radiographs, photographs, and photomicrographs. This database served as both a case submission portal and the archive of data and sample images (photographs, radiographs, and photomicrographs) of human calvarial osseous injuries at varying points of healing for the subsequent objectives of this study. In order to populate this database,

methods for sampling, decalcifying, and creating slides of fracture histomorphology were also developed, including sub-studies on decalcification agent and stain utility.

The second goal of this study was to microscopically evaluate the histological environment of cranial injury samples to ascertain the progression of tissues and cells during osseous repair in the outer table, diploë, and inner table of the cranium. As there is currently no widely accepted method for analyzing fracture histomorphology of human cranial bone, various premises were tested to ascertain the best materials and methods to produce histological slides that highlight the cells and tissues of cranial fracture healing. This included exploring the effects of different decalcification agents on length of decalcification and resulting quality of histologic specimens, the efficacy of four common stains in visualizing cranial histomorphology, and evaluations of interobserver error in the method developed for histological feature assessment.

The final aim of this research was to explore the process of fracture repair in the calvarium based upon the presence of tissue and cellular healing characteristics at different times. Correlation of these stages with the known fracture ages of the working sample produced the first scientifically validated model of healing in the human cranium, providing the foundation for a method to estimate the age of cranial injuries.

The project summaries, participants, design alterations, and outcomes of each research goal will be discussed independently.

Research Goal 1: Develop a Database of Cranial Fractures of Known Age

Research Design, Methods, and Analytical and Data Analysis Techniques

The Repository of Antemortem Injury Response (REPAIR) was designed to serve as an online case submission portal and repository of cranial injuries of known age for forensic case

comparison and future research. Throughout the course of the grant, the databank's utility and workflow were improved based on user feedback. Notable improvements include developing an approval queue for case submissions allowing administrators to screen for identifying decedent data prior to cases becoming visible to users, implementing data exportation to a *csv* file for data analysis, and creating a registration link for interested practitioners and contributors to request database access.

Samples of cranial injuries of known age to populate REPAIR were collected from medical examiner cases at Western Michigan University Homer Stryker M.D. School of Medicine's (WMed) Forensic and Autopsy Service, WMed's Body Donation Program, and partnering medical examiner offices. If possible, photographs and radiographs of the cranial injury were documented via photographs and radiographs. Excised samples were fixed in 10% neutral buffered formalin for two to four weeks, depending on the size and thickness of the specimen. Following fixation, the weight and dimensions of each sample were recorded, and pre-decalcification radiographs were taken at settings of 50 KVp and 2.5 mAs for adult samples and 40 to 48 KVp and 0.9 to 1.8 mAs for infant cranial bone and non-diploic adult bone. Samples were immersed into either neutral 10% Ethylenediaminetetraacetic acid (EDTA), 5% nitric acid, or 7% hydrochloric acid (HCl) until radiography confirmed complete extraction of bone minerals. Specimens immersed in EDTA were assessed radiographically every 20 days or less, in under 10 days for nitric acid samples, though typically in two- to three-day periods, and checked every one or two days for HCl. Decalcification solutions were changed at each radiographic assessment. To assess the impact of different decalcification agents on the resulting quality fracture histomorphology features, a decalcification study was completed.

When completely demineralized, the samples were rinsed under running water for at least one hour and cross-sections of the injury were cut, photographed, and placed into cassettes for paraffin embedding. Embedded samples were cut into four 4-6 μm thin sections on a microtome. Samples were affixed to microscopic slides and stained with hematoxylin and eosin (H&E), Masson's trichrome, alcian blue hematoxylin with an orange G counterstain (AB/OG), and Russell-Movat pentachrome. Each slide was checked microscopically for quality and recut or restained if not sufficient. Slides were digitally scanned at 40X using an Aperio CS2 digital slide scanner and archived in the Aperio e-slide management database. Each digital slide was also checked for quality. From these scans, images of the overall sample and magnified views of the outer table, diploë, and inner table were acquired and manually uploaded to the Photomicrographs section of REPAIR. Glass slides were compiled into slide sets consisting of the four differently stained slides for each sample.

Expected Applicability of the Research

Beyond being a repository of data related to this research, REPAIR serves as a valuable resource for forensic practitioners to use to compare cranial fractures of unknown age in forensic cases to those in this study. Furthermore, REPAIR is a foundational dataset for future researchers to explore new questions related to cranial fracture healing. Finally, REPAIR was designed to allow for the inclusion of postcranial fractures in future research endeavors, adding to its future utility.

Participants and Other Collaborating Organizations

For the design of the database, we worked with Occupational Research and Assessment (ORA) to design and host REPAIR and implement suggested improvements. Samples of cranial

injuries for the study were provided by Western Michigan University Homer Stryker M.D. School of Medicine (WMed) Forensic and Autopsy Service and WMed's Body Donation Program which were acquired by the PIs. Partner institutions that provided samples include the Pima County Office of the Medical Examiner in Tucson, Arizona, and the Macomb County Medical Examiner in Mt. Clemens, Michigan. Paraffin embedding, thin sectioning, mounting, and staining of glass slides were completed by histotechnologists Kristi Bailey and Jon Langworthy. The population of REPAIR with data and images was completed by the PIs, Kerianne Armelli, and Erica Christensen. All other tasks were completed by the PIs.

Design Alterations

To increase the participation of partnering institutions, an optional consent process and standard language for sample donation was developed for decedent next-of-kin. These changes were submitted to WMed's Institutional Review Board but the project remained "Not Human Subjects Research." A Grant Adjustment Notification (ID# 1061401) and updated Privacy Certificate were also submitted to the NIJ. After this change was approved on December 19, 2018, partnering institutions could contact the PIs to obtain a verbal consent from the decedent's next-of-kin for sample procurement.

Initially, this study included five histological stains: H&E, Masson's Trichrome, AB/OG, Perl's Prussian Blue (iron stain), and Tartrate-Resistant Acid Phosphatase (TRAP). Upon evaluations by the PIs, Perl's Prussian blue and TRAP were not performing in the manner expected. The iron stain failed to highlight its target protein, hemosiderin, and the TRAP stain chosen for its ability to highlight osteoclastic enzymes did not signal as anticipated. Both stains were discontinued from use in this study following failed efforts at troubleshooting. Russell-

Movat pentachrome was the chosen alternative for the discontinued stains as it distinguishes types of collagen, connective tissues, cartilage, bone, osteoid, and osteogenic cells.

Activities/Accomplishments

The Repository of Antemortem Injury Response is accessible at repair.orainc.com (Fig. 1) and includes a Submission Worksheet (Fig. 2) for case/decedent information, injury circumstances, and sample information; a Processing Worksheet (Fig. 3) detailing the specifics of the sample decalcification; and a Documentation section (Fig. 4) for radiographs, photographs, and photomicrographs of each specimen. The Advanced Search feature (Fig. 5) allows users to customize their search using any of the case information reflected within the worksheets and the administrators can export the data of interest for research purposes.

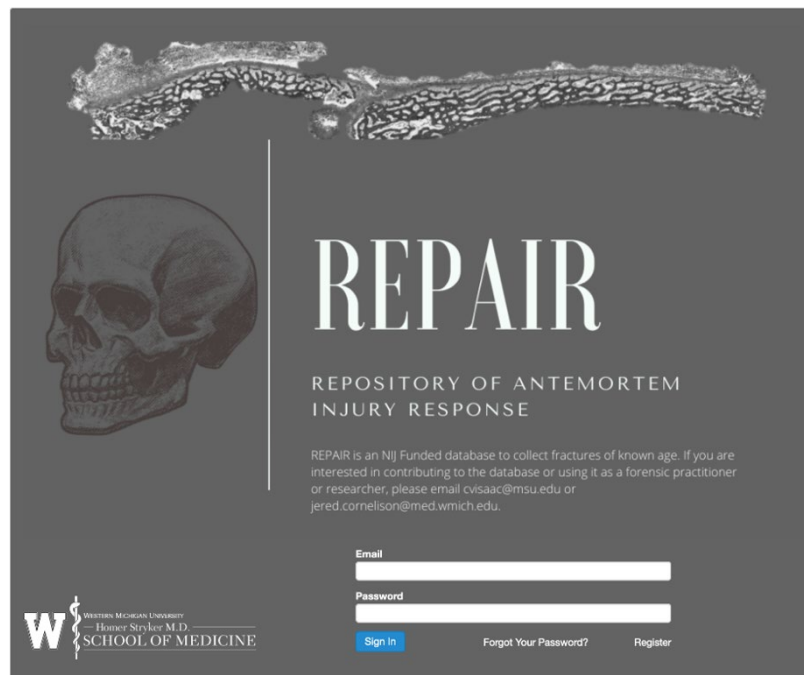


Figure 1. The Repository of Antemortem Injury Response (REPAIR) online case submission, comparison, and research database

The screenshot displays the REPAIR Submission Worksheet interface. At the top left is the Western Michigan University School of Medicine logo. At the top right is the Department of Pathology Repository of Antemortem Injury Response logo and a search bar. The main content area is divided into several sections:

- Home Menu:** Includes links for My Profile, Sign Out, My Cases, All Cases, and My Pending.
- Case:** Includes links for Submission Worksheet, Processing Worksheet, Evaluation Worksheet, and Chronology Report.
- Documentation:** Includes links for X-rays (8), Photomicrographs (28), Photographs (8), and Documents (1).
- Advanced Search:** Includes links for New Search, Revise Search, Last Search Results, and Saved Searches.
- Administration:** Includes a link for Permission Sets.

The main form area contains the following sections:

- Case Information:** Fields for Sex (Male), Age Yrs (54), Mths, Days, Date of death (06/10/2017), Date classifier (On), Race (White), Time of death (00:00), Time classifier (Exact), Organ procurement (No), and Date of autopsy (06/12/2017).
- Medical Conditions:** Checkboxes for Diabetes, Malnutrition, Infection, Unknown, Hypothyroidism, Peripheral vascular disease, Post-menopausal, Other (checked), Anemia, Alcoholism (checked), Osteoporosis, and Other description (non-Hodgkin's lymphoma).
- Medications:** Checkboxes for NSAIDs, Unknown, Corticosteroids, and Anticoagulants.
- Injury Circumstances:**
 - Injury Circumstance 1:** Date of injury (06/05/2017), Time of injury (00:00, Approximate), Cause of injury (Fall), Fall height (6 ft), Minimum number of impacts, Medical record of injury (Yes), Impact site (Anterior, Posterior, Right side (checked), Left side, Superior, Inferior, Unknown, Other).
 - Fracture Imaging:** Checkboxes for Antemortem X-ray, Postmortem X-ray, Antemortem CT, and Postmortem CT.
 - Bones affected:** Checkboxes for Frontal, Left parietal, Right parietal, Left temporal, Right temporal (checked), Left sphenoid, Right sphenoid, Occipital, and Other.
 - Surgical intervention:** No.
- Sample 1:** Location (Right temporal), Photographs (Overall fracture (checked), After removal, Detail of removed sample, Other), Fracture type (Linear (checked), Comminuted, Diastatic, Other), and Placed in formalin same day as autopsy? (checkbox).

Figure 2. Submission Worksheet in REPAIR containing case information related to the decedent, injury circumstances, and details of the sample taken for the study.

Case: FH-004 Welcome Test User

Home Menu

- My Profile
- Sign Out

Cases

- My Cases
- All Cases
- My Pending

Case

- Submission Worksheet
- Processing Worksheet**
- Evaluation Worksheet
- Chronology Report

Documentation

- X-rays (8)
- Photomicrographs (28)
- Photographs (8)
- Documents (1)

Advanced Search

- New Search
- Revise Search
- Last Search Results
- Saved Searches

- Injury Circumstance 1

- Sample 1

Location: Right temporal Placed in formalin same day as autopsy?

Photographs

Overall fracture After removal Detail of removed sample Other

Fracture type

Linear Depressed Comminuted Diastatic Other

Specimen 1a

Study Sample #	Decalcification start	Decalcification end
35	04/03/2018	05/08/2018
Decalcification time	Decalcification agent	X ray settings
35 days	EDTA	54.0 kVp 1.4 mAs
Weight	Length	Width
3.776 g	56.22 mm	16.59 mm
Thickness	Volume	
3.26 mm	3040.57 mm ³	

Figure 3. Processing Worksheet in REPAIR containing details of the sample dimensions and decalcification process.

Case: FH-044 Welcome Test User

Home Menu

- My Profile
- Sign Out

Cases

- My Cases
- All Cases
- My Pending

Case

- Submission Worksheet
- Processing Worksheet
- Evaluation Worksheet
- Chronology Report

Documentation

- X-rays (18)
- Photomicrographs (40)**
- Photographs (21)
- Documents (1)

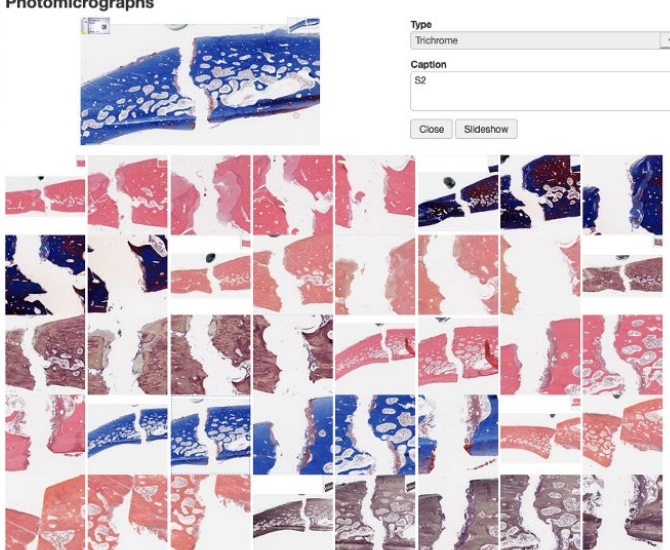
Advanced Search

- New Search
- Revise Search
- Last Search Results
- Saved Searches

Administration

- Permission Sets

Photomicrographs



Type: Trichrome

Caption: S2

Close Slideshow

Figure 4. Photomicrograph section of the Documentation tab with images of the four differently stained histology slides.

The screenshot displays the REPAIR web application interface. At the top left is the Western Michigan University School of Medicine logo. At the top right is the Department of Pathology Repository of Antemortem Injury Response logo and a search bar. Below the logos is a navigation menu with sections: Home Menu (My Profile, Sign Out), Cases (My Cases, All Cases, My Pending), Advanced Search (New Search, Revise Search, Last Search Results, Saved Searches), and Administration (Permission Sets). The main content area is titled 'Build a Search' and contains a table with columns: Form, Field, Option, and Value. The table lists search criteria: Case Information (Age year, equal to, 3), Injury Circumstances (Injury Age days from death, equal to, 21), Samples (Fracture type linear, is, Checked), and Injury Circumstances (Surgical intervention, contains any, No). Below the table is a 'Search' button and a list of expandable categories: Case Information, Medical Conditions, Medications, Injury Circumstances, Surgical Interventions, Samples, and Specimens.

Figure 5. Customizable search capabilities of REPAIR.

Results and Findings

The Repository of Antemortem Injury Response currently houses 86 case files of individuals aged 20 days to 87 years (Table 1) with 187 samples of fractures and medical interventions to the calvarium of known ages ranging from acute to 46 years of healing (Table 2). Table 3 provides a summary of the macroscopic injury types represented within REPAIR.

Table 1. REPAIR cases and samples by age group

AGE GROUP	DECEDENT CASES	SAMPLES
Infant (0-3 years)	10	25
Juvenile (3-16 years)	4	12
Adult (16+ years)	72	150
TOTAL	86	187

Table 2. REPAIR sample cranial injury ages

INJURY AGES	SAMPLES
Acute	19
<1 day	12
1-7 days	43
8-30 days	20
31-90 days	16
91-365 days	11
365-1825 days (1-5 years)	12
>1825 days (>5 years)	48
Unknown	6
TOTAL	187

Table 3. REPAIR cranial injury types to date

INJURY TYPES	SAMPLES
Linear	80
Craniotomy/Craniectomy/Cranioplasty	45
Diastatic	16
Burr hole	15
Depressed	9
Ventriculoperitoneal (VP) Shunt	6
Cephalohematoma	5
Comminuted	4
Suture	3
Intracranial Pressure Monitor	2
Hinge	1
None	1
TOTAL	187

Research Goal 1a: Decalcification Agent and Sample Preservation

Research Design, Methods, Analytical and Data Analysis Techniques

This sub-study had two components. The first was to assess the variables that influence the time it takes to decalcify a sample and the second was to assess the visibility of fracture histomorphology features of samples decalcified with different agents. For the first portion of the study, 124 samples (Table 4) were used to calculate and discern sample characteristics

contributing to decalcification time, including decedent age and sample dimensions.

Measurements of sample thickness, width, and length were available for 113 of the 124 samples; volume and surface area were calculated for these samples (Table 5). All samples were fixed in 10% neutral buffered formalin for two to four weeks and decalcified in either 10% EDTA ($n=34$), 5% nitric acid ($n=83$), or 7% hydrochloric acid ($n=7$) (Table 4) until radiographic assessment confirmed complete demineralization. Decalcification times were recorded in days.

Table 4. Samples per decalcification agent by age group

AGE GROUP	DECALCIFICATION AGENT			
	EDTA	HCL	NITRIC ACID	TOTAL
Infant	7	2	7	16
Juvenile	5	1	4	10
Adult	22	4	72	98
Total	34	7	83	124

Table 5. Sample measurements

	N	MEAN	STD DEV	MIN	LOWER QUARTILE	MEDIAN	UPPER QUARTILE	MAX
Age of Decedent (years)	124	39.7	25.1	0.2	22.6	39.2	60.9	87.8
Sample length (mm)	113	42.2	17.1	11.9	32.0	38.2	50.3	122.3
Sample width (mm)	113	27.7	12.7	6.1	20.1	26.7	33.5	88.7
Sample thickness (mm)	113	7.9	3.5	1.5	5.4	7.5	9.9	24.0
Calculated Volume (mm ³)	113	11268.4	13977.2	198.8	3672.6	7833.1	13564.5	104160.6
Calculated Surface Area (mm ²)	113	3761.5	3127.2	253.0	2156.8	3138.6	4766.6	23142.6
Decalcification time (days)	124	28.9	45.4	1	7	11	24.5	281

Decalcification times for each agent were analyzed visually and through averages to assess expediency and distribution. A general linear model to predict decalcification time from dimensional variables, decedent age, and decalcification agent was developed through a step-up modeling process. The base model consisted of decalcification agent, EDTA or nitric acid, as the single predictive variable of processing time. HCl was discontinued because of the poor quality of the resulting slides, thus it was excluded from inferential analysis due to its underrepresentation within the sample set. The heteroscedascity of the initial modelling process was removed through the log transformation of the response variable and the modelling process was restarted using log-time as the outcome measure. Type-III sum-of-squares p-values at a significance level of 5% were used to evaluate models. To evaluate the difference between the model's estimated predicted value and the true observed time, log-time to time transformed residual values were analyzed. The log-time residuals were exponentiated and applied as a multiplicative factor to the corresponding observed decalcification times, providing residual values for predicted time.

To assess histological slide quality, six formalin-fixed fracture samples were cut into three sections for decalcification in 10% EDTA, 5% nitric acid, and 7% hydrochloric acid respectively. The resulting 18 demineralized samples were used to create slides stained with hematoxylin and eosin. Seven evaluators with expertise in histology assessed the preservation of each slide's tissues, cells, and nuclei using a Likert scale from one to five in order of increasing feature quality and clarity.

Generalized linear mixed models using an ordered multinomial response variable and cumulative logit linking function were used to assess Likert scores for tissues, cells, and nuclei. Decalcification agent was the fixed effect and sample identifier and evaluator were assessed as

covariates. These covariates were assessed due to preliminary analysis of the data indicating certain evaluators scored samples higher regardless of histological feature or decalcification agent, and particular samples scored high in every possible category while others were scored low. Odds ratios were produced for each histological feature for three comparisons: EDTA vs. nitric acid, nitric acid vs. HCl, and EDTA vs. HCl. The non-normal distribution of Likert scores and apparent influence of evaluator and sample identifier upon scoring necessitated the use of a Bonferroni-corrected p-value of 0.0167 to control for type-1 errors. P-values between 0.0167 and 0.05 were deemed “borderline significant”.

Expected Applicability of the Research

This study was conducted to provide useful data for practitioners to determine which decalcification agent to use based on the decedent’s age, sample dimensions, and time constraints compared to the resulting slide quality.

Participants and Other Collaborating Organizations

Evaluations were completed by the seven project evaluators. The data analysis was completed by biostatistician Joseph Billian. The sample preparation and data collection were completed by PI Jered Cornelison.

Results and Findings

HCl provided the fastest decalcification (\bar{X} =3.57 days), followed by nitric acid (\bar{X} =10.35 days), then EDTA (\bar{X} =78.97 days). However, EDTA decalcified samples over a broader range of times than its acidic counterparts (Table 6). Decalcification time in HCl and nitric acid varied little between age cohorts (Table 7), while decalcification time in EDTA was reduced for infants.

Figure 6 highlights the variation in EDTA decalcification time with age and the underrepresentation of HCl samples, prompting exclusion of HCl from the inferential analysis.

Table 6. Agent decalcification rates

DECALCIFICATION AGENT	$\bar{X} \pm SD$ (DAYS)	MAX (DAYS)	MIN (DAYS)	RANGE (DAYS)
10% EDTA	78.97 \pm 63.13	281	4	277
5% Nitric Acid	10.35 \pm 5.54	30	1	29
7% HCl	3.57 \pm 2.70	9	1	8

Table 7. Decalcification rate in days by age cohort

AGE GROUP	DECALCIFICATION AGENT	N	MIN	MAX	MEAN	STD DEV
Infant (0-3 yrs)	EDTA	7	4	53	16.71	18.25
	Nitric	7	1	24	7.14	7.67
	HCL	2	1	4	2.50	2.12
Juvenile (3-16 yrs)	EDTA	5	60	108	74.6	19.67
	Nitric	4	5	9	7	1.83
	HCL	1	3	3	3	--
Adult (16+ years)	EDTA	22	25	281	99.77	65.91
	Nitric	72	3	30	10.85	5.33
	HCL	4	1	9	4.25	3.40

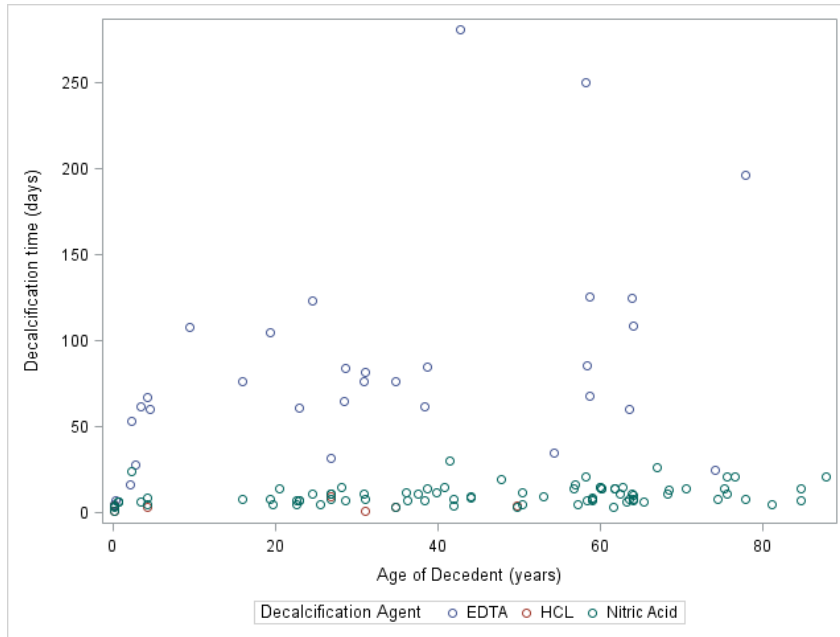


Figure 6. Scatter plot of decalcification time versus decedent age in years.

The general linear model derived from the step-up modeling process for decalcification time (Equation 1) included decedent age, decalcification agent, sample thickness, and sample width as statistically significant predictive elements. When controlling all variables except agent, decalcification time is 3.1 times greater for EDTA than nitric acid. The effect size of the prediction variables, as indicated by their coefficient values, is greater for EDTA, except for sample width.

Equation 1. General linear model for the prediction of decalcification time in logTime and Time in days

$$\log Time = \begin{cases} 2.144 + 0.016 * age + 0.174 * thickness + 0.017 * width : decal = EDTA \\ 1.009 + 0.004 * age + 0.062 * thickness + 0.017 * width : decal = Nitric Acid \end{cases}$$

$$Time = \begin{cases} 8.534 * 1.016^{age} * 1.190^{thickness} * 1.017^{width} : decal = EDTA \\ 2.742 * 1.004^{age} * 1.064^{thickness} * 1.017^{width} : decal = Nitric Acid \end{cases}$$

Increasing decedent age by one year increased decalcification time in EDTA by 1.6% and 0.4% in nitric acid. Age-agent interaction was insignificant ($p=0.17$) for nitric acid and

significant ($p=0.01$) for EDTA. Sample thickness had a greater impact upon EDTA than nitric acid with 19% and 6.4% increases in decalcification time respectively at a 1 mm increase in thickness. The decal-thickness interaction was significant for both EDTA ($p=0.0007$) and nitric acid ($p=0.0038$). Sample width did not have a differential effect between agents.

Transformed residual values indicating model precision are shown in Table 8. Accuracy was not calculated as the sample was not partitioned prior to model development to allow for scoring.

Table 8. Transformed residuals of the general-linear model

Percentile	Transformed Residual
0%	-132.1 days
5%	-21.8 days
25%	-2.8 days
50%	0.3 days
75%	3.9 days
95%	42.6 days
100%	75.4 days

Regarding sample quality, EDTA decalcification produced the highest average Likert scores in every feature category (tissue, cells, and nuclei), followed by nitric acid and HCl (Table 9). Covariance estimates for the tissue model were 2.1 (SE=1.5) for evaluator and 2.4 (SE=1.7) for sample identifier. Cells model covariance estimates for evaluators and samples were 0.4 (SE=0.4) and 3.4 (SE=2.3), respectively, and the nuclei model had covariance estimates of 1.2 (SE=0.8) for evaluator and 2.7 (SE=1.8) for sample identifier.

Table 9. Likert Scores

RANK	DECALCIFICATION AGENT	MEAN ± STANDARD DEVIATION		
		TISSUES	CELLS	NUCLEI
1	EDTA (<i>n</i> =42)	4.1 ± 0.9	3.7 ± 1.0	3.7 ± 1.2
2	Nitric acid (<i>n</i> =42)	3.8 ± 1.1	3.4 ± 1.2	3.2 ± 1.3
3	HCl (<i>n</i> =42)	3.6 ± 1.0	3.0 ± 1.3	2.9 ± 1.3

Based on odds ratios (Table 10), EDTA is significantly more likely to receive a higher Likert score than HCl for all features. EDTA is also likely to score higher in all features when compared to nitric acid, but this is borderline significant for tissues ($p=0.0462$) and nuclei ($p=0.0117$) and not significant for cells ($p=0.1515$).

Table 10. Likert Score Odds Ratios

COMPARISON	TISSUES	CELLS	NUCLEI
EDTA (1) vs. Nitric (2) (p-value)	2.4 * (0.0462)	1.8 (0.1515)	2.7 * (0.0177)
Nitric (2) vs. HCl (3) (p-value)	1.5 (0.3597)	2.5 * (0.0285)	1.8 (0.1354)
EDTA (1) vs. HCl (3) (p-value)	3.7 ** (0.0048)	4.6 ** (0.0006)	5.1 ** (0.0003)

*Borderline significant ($0.0167 < p \leq 0.05$)

**Significant ($p \leq 0.0167$)

Decalcification in EDTA produces the highest sample quality of the three decalcification agents but is the most time-consuming. Nitric acid produces swift decalcification with good sample preservation for adult and juvenile specimens and bone thicker than 3 mm. However, thin samples of the cranial vault (<3 mm) from infants and children ages birth to three years are best decalcified in EDTA which provides the best preservation in a time comparable to nitric acid.

Research Goal 2: Evaluate Histological Environment of Fracture Sample

Research Design, Methods, Analytical and Data Analysis Techniques

Seven evaluators (one anatomist and six forensic pathologists) with extensive histology experience were employed to assess 154 sample slide sets, with each set containing four differently stained slides of the same sample (Table 11). Each set was assigned three randomly selected evaluators. Slides were assessed under a microscope or with the scanned digital slides using the Histology Sample Evaluative Form (Fig. 7) developed for the project. Each evaluator completed a form for every stain at all three anatomic zones (outer table, diploë, inner table), producing 12 assessments of a single injury sample per evaluator. Upon completion of the forms and review by the project administrators for errors or missing data, evaluation worksheets were entered into the online database Research Electronic Data Capture (REDCap).

Table 11. Samples evaluated by three observers.

AGE GROUP	DECEDENT CASES	SAMPLES
Infant (0-3 years)	7	16
Juvenile (3-16 years)	4	7
Adult (16+ years)	68	131
TOTAL	80	154

HISTOLOGY SAMPLE EVALUATIVE FORM FH #: _____ Evaluator: _____ Injury Type: _____

DECALCIFICATION METHOD (circle one) EDTA Nitric HCL STAIN (circle one): H&E Trichrome ABH/orange G Pentachrome
 ZONE (circle one): Outer Table Diploë Inner Table

FEATURE	Sub-feature		Circle One	Details	Notes
HEMATOMA	Y	N			
Organization	Y	N		If Y, EXTENT: Minimal Mild Moderate Extensive	
Pigment-Laden Macrophages	Y	N		If Y, EXTENT: Minimal Mild Moderate Extensive	
Fibrin	Y	N		If Y, EXTENT: Minimal Mild Moderate Extensive	
INFLAMMATION	Y	N		If Y, INFL. TYPE: Acute Chronic Mixed	
				If Y, INTENSITY: Mild Moderate Severe	
				If Y, DISTRIBUTION: Focal Patchy Widespread	
FRACTURE EDGE	Sharp	Blurred	N/A		
CONNECTIVE TISSUE	Y	N			
Mesenchyme/Loose C.T.	Y	N		If Y, EXTENT: Minimal Mild Moderate Extensive	
Fibroblasts/cytes	Y	N		If Y, FREQUENCY: Rare Mild Moderate Extensive	
Fibrous C.T./collagen	Y	N		If Y, EXTENT: Minimal Mild Moderate Extensive	
NEW CAPILLARIES	Y	N		If Y, EXTENT: Minimal Mild Moderate Extensive	
CARTILAGE FORMATION	Y	N			
Cartilage matrix	Y	N		If Y, EXTENT: Minimal Mild Moderate Extensive	
BONE FORMATION/REMODELING	Y	N			
Bone matrix	Y	N		If Y, EXTENT: Minimal Mild Moderate Extensive	
Bone Resorption	Y	N			
Woven Bone	Y	N		If Y, EXTENT: Minimal Mild Moderate Extensive	
Lamellar Bone	Y	N		If Y, EXTENT: Minimal Mild Moderate Extensive	
Reversal/Cement Lines	Y	N			

MSC – mesenchymal stem cells. C.T. – Connective tissue

Figure 7. Histology sample evaluative form

Research Goal 2a: Interobserver Error

Research Design, Methods, Analytical and Data Analysis Techniques

A preliminary interobserver error test was undertaken to evaluate the reliability of the method for analyzing the fracture histomorphology of the human cranial vault and determine any required adjustments. Interobserver error was assessed according to stain type, anatomical zone, and healing feature using both an unadjusted kappa coefficient and Prevalence-Adjusted Bias-Adjusted kappa (PABAK), the latter of which accounts for agreement by chance and skewed data patterns. The study included 48-53 fracture samples. A 2-way analysis was utilized as most samples had only been assessed by two evaluators due to the preliminary nature of the data at the time of this study. Both the PABAK and unadjusted kappa values were interpreted using the bins outlined in Table 12⁷.

Table 12. Interobserver error kappa interpretation

KAPPA VALUE	INTERPRETATION
≤ 0.0	No agreement
0.01 – 0.20	None to slight
0.21 – 0.40	Fair
0.41 – 0.60	Moderate
0.61 – 0.80	Substantial
0.81 – 1.00	Almost perfect

Expected Applicability of the Research

This study was completed to ascertain whether the evaluation forms and the features on the forms could be identified in fractures samples by multiple observers for different stains and anatomic zones.

Results and Findings

For all assessments of interobserver error the PABAK values are greater than the unadjusted kappa values. This is expected as the raw evaluative data show a high prevalence of “not present” scores for many histological features. Unadjusted kappa values interpret the high incidence of absent scores as chance agreement, which is misleading for this study. PABAK accounts for the skewed data distribution and provides the better measure of agreement between observers.

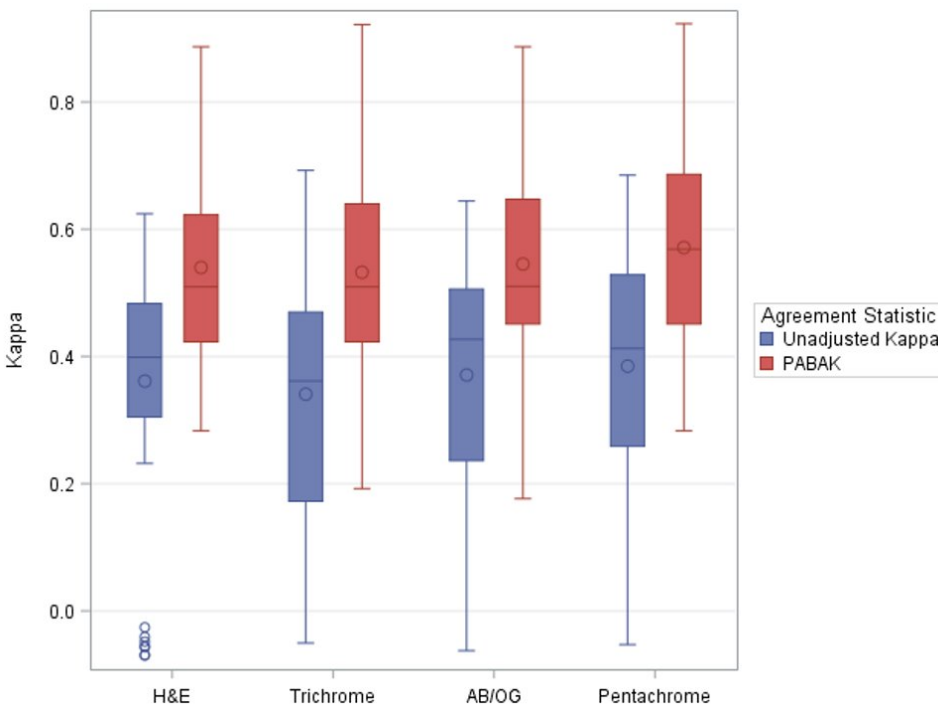


Figure 8. Interobserver error and histological stain

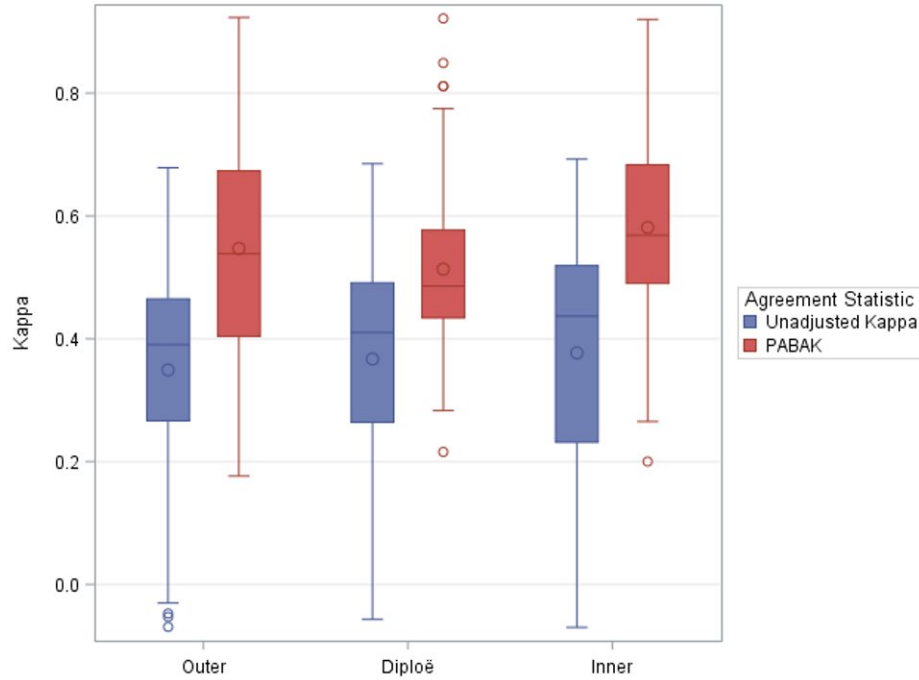


Figure 9. Interobserver error and anatomical zone

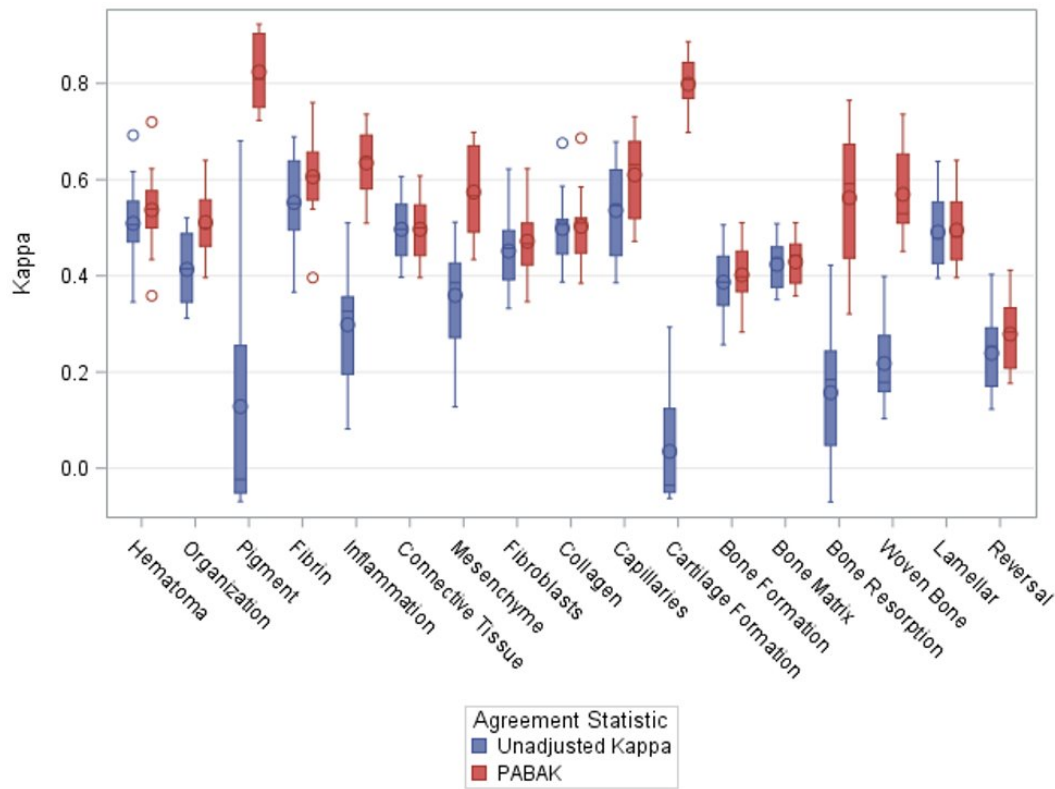


Figure 10. Interobserver error and histological feature

The mean PABAK values for observer agreement compared through the four histological stains, shown by the circles in Figure 8, all fell within the moderate agreement range. The PABAK values according to the anatomical zone (Fig. 9) also indicated evaluators are in moderate agreement on average. The interquartile ranges for both histological stain and anatomical zone PABAK values fell in the moderate to substantial agreement range.

As expected, the PABAK values for histological features varied (Fig. 10). Reversal/cement lines had the lowest average PABAK score in the fair agreement range. Hematoma, organization, connective tissue, mesenchyme, fibroblasts/cytes, collagen, bone formation, bone matrix, bone resorption, woven bone, and lamellar bone were on average in moderate agreement. There was substantial agreement between evaluators for fibrin, inflammation, new capillaries, and almost perfect agreement for pigment-laden macrophages and cartilage formation. Overall, interpretation of the PABAK values indicate the technique is a viable method for assessing the fracture histomorphology of the human cranial vault.

Research Goal 2b: Staining and Cranial Histology

Research Design, Methods, Analytical and Data Analysis Techniques

Histological slide sets for cranial fractures were developed using the stains hematoxylin and eosin (H&E), Masson's trichrome, alcian blue with an orange G counterstain (AB/OG), and Russell-Movat pentachrome. Four sets of histological slides, corresponding with the four stains, from 154 fracture/injury samples were reviewed by three evaluators for the presence, extent, and character of the features and sub-features associated with fracture repair as reflected in the Histology Sample Evaluative Form (Fig. 7). Assessments were done separately for each of the

four stains at the outer table, diploë, and inner table, and evaluators were asked to provide comments on their ability to see each histological feature with a given stain.

The level of agreement between evaluators for the absence/presence and extent of the histological features of healing for each of the four stains was evaluated using a 3-way kappa test. Kappa3 scores for the outer table, diploë, and inner table were condensed by taking the highest score between the zones for each feature and stain combination for each sample. To select the best stains for each histological feature, mean kappa values were aggregated across zones for each feature and stain. Each average was sectioned into bins outlining the greatest level of agreement between observers to prevent any overvaluation of small differences in kappa values (Table 12)⁷.

Expected Applicability of the Research

This research was done to identify which histological stains would be best for investigating the features of fracture histomorphology.

Design Alterations

Due to the coronavirus pandemic, histological slide evaluations could no longer be completed on the physical slide sets with microscopes. To address this issue, a fillable pdf evaluation form was developed, and the scanned digital slide sets from the Aperio CS2 scanner were distributed to evaluators. Assessment results were entered into the REDCap database as previously done for the physical assessments.

Results and Findings

The results of the kappa3 analysis for interobserver agreement of the four histological stains (H&E, Masson's trichrome, AB/OG, and Russell-Movat pentachrome) are presented in Table 13. Fibrin was the only feature for which a single stain produced the highest level of agreement. The 17 other features had either a two, three, or four-way tie between stains for the highest level of agreement. For example, bone formation/remodeling's kappa scores for the four stains were all within the fair agreement range (0.21 – 0.39). The raw kappa value was highest for pentachrome ($\kappa = 0.38$); however, the lowest kappa score, associated with AB/OG ($\kappa = 0.34$), was still within the fair agreement range, thus the difference in visualizing bone formation/remodeling between all four stains is negligible.

The results indicate there was no single stain which allowed investigators to comprehensively assess the presence/absence of all 18 features and sub-features of fracture repair. For most features, there was fair agreement between the evaluators' assessments using any of the four stains. The only exception is for fibrin where kappa values indicate evaluators agreed to a substantial degree ($\kappa = 0.61-0.80$) in either the absence or presence of fibrin using the trichrome stain.

Table 13. Level of observer agreement for stains using kappa3. Stain code: hematoxylin and eosin (H&E), trichrome (TriChr), alcian blue hematoxylin/orange G (AB/OG), pentachrome (PChr)

HEALING FEATURE	GREATEST LEVEL OF AGREEMENT	# OF STAINS AT LEVEL OF AGREEMENT	DECREASING RAW KAPPA3 VALUE			
			Stain 1	Stain 2	Stain 3	Stain 4
Bone Formation/Remodeling	Fair	4	PChr	H&E	TriChr	AB/OG
Bone Matrix	Fair	4	TriChr	PChr	H&E	AB/OG
Bone Resorption	Fair	4	PChr	AB/OG	H&E	TriChr
Capillaries	Moderate	4	TriChr	H&E	PChr	AB/OG
Cartilage Formation	Fair	3	PChr	TriChr	AB/OG	
Collagen/Fibrous C.T.	Substantial	2	AB/OG	PChr		
Connective Tissue	Moderate	4	AB/OG	PChr	TriChr	H&E
Fibrin	Substantial	1	TriChr			
Fibroblasts/cytes	Moderate	4	H&E	AB/OG	PChr	TriChr
Fracture Edge Blurred	Fair	4	TriChr	H&E	AB/OG	PChr
Hematoma	Moderate	4	AB/OG	TriChr	H&E	PChr
Inflammation	Fair	4	TriChr	H&E	AB/OG	PChr
Lamellar Bone	Fair	4	TriChr	H&E	AB/OG	PChr
Mesenchyme/Loose C.T.	None to slight	4	AB/OG	PChr	TriChr	H&E
Organization	Moderate	4	TriChr	H&E	PChr	AB/OG
Pigment-Laden Macrophages	Fair	2	TriChr	PChr		
Reversal Lines	Fair	2	H&E	PChr		
Woven Bone	Fair	4	H&E	TriChr	PChr	AB/OG

Research Goal 2c: Features and Stages of Cranial Vault Fracture Healing

Research Design, Methods, Analytical and Data Analysis Techniques

To elucidate the histological progression of healing in the human cranial vault, only samples having an exact and confirmed time since injury were utilized in this portion of the study (Table 14). Due to limited samples for infants ($n=15$) and juveniles ($n=7$), continued inferential analyses were performed on the adult sample only ($n=125$). However, qualitative observations of the differences of infant and juvenile cranial repair from adult healing were made. For each adult sample, the presence/absence of each feature in each zone was determined

with a majority rule ($\geq 50\%$) using the evaluations from the stain(s) achieving the highest level of interobserver agreement for each feature (see results of “Research Goal 2b: Staining and Cranial Histology”). Samples were partitioned into healing time categories outlined in Table 15. The presence of each histological feature in each healing time category was assessed.

Table 14. Samples with known age of injury

AGE GROUP	DECEDENT CASES	SAMPLES
Infant (0-3 years)	6	15
Juvenile (3-16 years)	4	7
Adult (16+ years)	68	125
TOTAL	78	147

The extent variable was explored for the following features of healing in adults: hematoma organization, fibrin, fracture edge, mesenchyme/loose connective tissue, fibroblasts/cytes, fibrous connective tissue/collagen, new capillaries, and lamellar bone. Evaluations for samples were coded to correspond with the absence/presence and level of extent for each feature. For example, evaluations of hematoma organization were scored on the following scale: 0 = ‘absent’, 1 = ‘minimal’, 2 = ‘mild’, 3 = ‘moderate’, and 4 = ‘extensive’. The scores were averaged for each zone of a sample and aggregated across the different stains and evaluators. These extent variables as well as inflammation type, intensity, and distribution, cartilage, and woven bone were explored on a sample-by-sample basis for infant and juvenile specimens.

Table 15. Healing time categories for adult samples

HEALING TIME	SAMPLES
Acute	10
0-1 hours	5
1-24 hours	4
1-7 days	29
7-14 days	8
14-30 days	6
1-6 months	7
6-18 months	10
18+ months	46
Total	125

Co-occurrence of healing features in adults was examined using Yule's Q. Analyses were completed for the entire adult sample ($n=125$) using every histological feature without regard to healing time. Co-occurrence was also assessed within specific healing times for select features. Only the 1-7 days ($n=29$) and 18+ months ($n=46$) bins of fracture healing time (Table 15) had enough samples to perform a descriptive analysis of co-occurrence. Within the two bins of interest, features with occurrence rates of 10-90% were assessed. Nine features were examined for samples with 1-7 days of healing time: hematoma, organization, fibrin, inflammation, fracture edge (blurred), connective tissue, fibroblasts, collagen, and bone formation. Seven features were examined for samples with 18+ months of healing time: connective tissue, fibroblasts, collagen, capillaries, bone resorption, woven bone, and reversal.

Expected Applicability of the Research

This research was done to assess the progression of histological features of healing in the cranial vault. It identifies the presence, extent, and cooccurrence of 18 histological features for future use in developing a method to date fractures of the calvarium.

Participants and Other Collaborating Organizations

Evaluations were completed by the project's 7 evaluators. Data analysis of histological feature presence and extent was completed by biostatistician Joseph Billian.

Results and Findings

Amongst the sample of adult cranial vault injuries, cartilage and pigment-laden macrophages were almost entirely absent, occurring in less than 2% of all samples. Inflammation produced present score frequencies of less than 10% for all anatomical zones. Woven bone was present in less than 15% of the samples for all three zones. Mesenchyme and bone resorption were identified in fewer than 20% of specimens in all zones. Notably, the absence of cartilage and woven bone from the fracture healing process indicates that adult cranial healing lacks both soft cartilaginous and hard woven bone callus stages that occur with postcranial healing. All other features of healing scored on an absent/present basis were observed in 20% or more of the sample. Table 16 shows the features present at different healing times for the adult sample.

Trends of when features appear, peak, and wane can be discerned from Table 16. In the 1-to-7-day range there is a peak in the presence of hematoma, hematoma organization, and fibrin. Between 7- and 14-days, connective tissue features become prevalent in the majority of samples, including mesenchyme, fibroblasts, and collagen. In the next time range, 14 to 30 days, these features peak and decrease thereafter. New capillaries also peak in the 14-to-30-day range

and blurred fracture edge and bone formation processes, in particular bone matrix and reversal lines, are seen in most samples. By 1 to 6 months, the bone formation features of bone matrix, lamellar bone, and reversal lines are present in over 75% of samples and remain so for the remainder of the healing process.

Table 16. Feature presence and healing time for adult sample.

Feature	Zone	n	Acute	0-1 hr	1-24 hr	1-7 d	7-14 d	14-30 d	1-6 mo	6-18 mo	18+ mo
TOTAL		125	10	5	4	29	8	6	7	10	46
Hematoma	O	37 (30%)	2 (20%)	1 (20%)	1 (25%)	23 (79%)	3 (38%)	3 (50%)	2 (29%)	1 (10%)	1 (2%)
	D	42 (34%)	4 (40%)	1 (20%)	1 (25%)	23 (79%)	2 (25%)	5 (83%)	1 (14%)	3 (30%)	2 (4%)
	I	41 (33%)	2 (20%)	1 (20%)	2 (50%)	23 (82%)	2 (25%)	3 (50%)	2 (29%)	2 (20%)	4 (9%)
Organization	O	27 (22%)	0 (0%)	1 (20%)	0 (0%)	20 (69%)	3 (38%)	2 (33%)	1 (14%)	0 (0%)	0 (0%)
	D	29 (23%)	1 (10%)	0 (0%)	0 (0%)	19 (66%)	2 (25%)	4 (67%)	1 (14%)	2 (20%)	0 (0%)
	I	26 (21%)	1 (10%)	1 (20%)	0 (0%)	18 (64%)	1 (13%)	2 (33%)	1 (14%)	1 (10%)	1 (2%)
Pigment	O	1 (1%)	0 (0%)	0 (0%)	0 (0%)	1 (3%)	0 (0%)	0 (0%)	0 (0%)	0 (0%)	0 (0%)
	D	1 (1%)	0 (0%)	0 (0%)	0 (0%)	1 (3%)	0 (0%)	0 (0%)	0 (0%)	0 (0%)	0 (0%)
	I	1 (1%)	0 (0%)	0 (0%)	0 (0%)	1 (4%)	0 (0%)	0 (0%)	0 (0%)	0 (0%)	0 (0%)
Fibrin	O	29 (23%)	1 (10%)	0 (0%)	0 (0%)	22 (76%)	2 (25%)	2 (33%)	1 (14%)	1 (10%)	0 (0%)
	D	37 (30%)	4 (40%)	0 (0%)	0 (0%)	22 (76%)	2 (25%)	4 (67%)	1 (14%)	2 (20%)	2 (4%)
	I	29 (23%)	1 (10%)	1 (20%)	0 (0%)	19 (68%)	2 (25%)	3 (50%)	1 (14%)	1 (10%)	1 (2%)
Inflammation	O	9 (7%)	0 (0%)	0 (0%)	0 (0%)	5 (17%)	1 (13%)	1 (17%)	1 (14%)	0 (0%)	1 (2%)
	D	10 (8%)	0 (0%)	0 (0%)	0 (0%)	7 (24%)	0 (0%)	1 (17%)	0 (0%)	1 (10%)	1 (2%)
	I	8 (6%)	0 (0%)	0 (0%)	0 (0%)	4 (14%)	0 (0%)	1 (17%)	1 (14%)	1 (10%)	1 (2%)
Fracture Edge Blurred	O	69 (55%)	1 (10%)	0 (0%)	0 (0%)	7 (24%)	3 (38%)	3 (50%)	6 (86%)	8 (80%)	41 (100%)
	D	70 (56%)	1 (10%)	0 (0%)	0 (0%)	7 (24%)	3 (38%)	4 (67%)	6 (86%)	8 (80%)	41 (100%)
	I	71 (57%)	1 (10%)	0 (0%)	0 (0%)	7 (25%)	3 (38%)	4 (67%)	5 (71%)	8 (80%)	43 (100%)
Connective Tissue	O	57 (46%)	1 (10%)	1 (20%)	0 (0%)	5 (17%)	5 (63%)	4 (67%)	4 (57%)	3 (30%)	34 (74%)
	D	56 (45%)	2 (20%)	0 (0%)	0 (0%)	5 (17%)	5 (63%)	5 (83%)	4 (57%)	4 (40%)	31 (67%)
	I	52 (42%)	0 (0%)	0 (0%)	0 (0%)	4 (14%)	4 (50%)	4 (67%)	4 (57%)	2 (20%)	34 (74%)
Mesenchyme	O	16 (13%)	0 (0%)	0 (0%)	0 (0%)	1 (3%)	4 (50%)	3 (50%)	3 (43%)	1 (10%)	4 (9%)
	D	21 (17%)	1 (10%)	0 (0%)	0 (0%)	2 (7%)	4 (50%)	3 (50%)	2 (29%)	2 (20%)	7 (15%)
	I	13 (10%)	0 (0%)	0 (0%)	0 (0%)	0 (0%)	2 (25%)	2 (33%)	2 (29%)	1 (10%)	6 (13%)
Fibroblasts/cytes	O	46 (37%)	0 (0%)	0 (0%)	0 (0%)	4 (14%)	5 (63%)	3 (50%)	4 (57%)	2 (20%)	28 (61%)
	D	47 (38%)	1 (10%)	0 (0%)	0 (0%)	3 (10%)	5 (63%)	5 (83%)	4 (57%)	3 (30%)	27 (59%)
	I	45 (36%)	0 (0%)	0 (0%)	0 (0%)	3 (11%)	4 (50%)	3 (50%)	4 (57%)	2 (20%)	29 (63%)
Collagen	O	54 (43%)	0 (0%)	1 (20%)	0 (0%)	5 (17%)	4 (50%)	4 (67%)	3 (43%)	3 (30%)	34 (74%)
	D	51 (41%)	1 (10%)	0 (0%)	0 (0%)	4 (14%)	4 (50%)	4 (67%)	4 (57%)	4 (40%)	30 (65%)
	I	49 (39%)	0 (0%)	0 (0%)	0 (0%)	4 (14%)	2 (25%)	4 (67%)	4 (57%)	2 (20%)	33 (72%)
	O	40 (32%)	0 (0%)	0 (0%)	0 (0%)	2 (7%)	4 (50%)	4 (67%)	4 (57%)	1 (10%)	25 (54%)

New Capillaries	D	47 (38%)	2 (20%)	0 (0%)	0 (0%)	3 (10%)	3 (38%)	5 (83%)	4 (57%)	4 (40%)	26 (57%)
	I	39 (31%)	0 (0%)	0 (0%)	0 (0%)	1 (4%)	2 (25%)	3 (50%)	4 (57%)	2 (20%)	27 (59%)
Cartilage Formation	O	1 (1%)	0 (0%)	0 (0%)	0 (0%)	1 (3%)	0 (0%)	0 (0%)	0 (0%)	0 (0%)	0 (0%)
	D	2 (2%)	0 (0%)	0 (0%)	0 (0%)	1 (3%)	0 (0%)	0 (0%)	0 (0%)	0 (0%)	1 (2%)
	I	1 (1%)	0 (0%)	0 (0%)	0 (0%)	1 (4%)	0 (0%)	0 (0%)	0 (0%)	0 (0%)	0 (0%)
Bone Formation	O	77 (62%)	0 (0%)	0 (0%)	0 (0%)	7 (24%)	3 (38%)	5 (83%)	7 (100%)	9 (90%)	46 (100%)
	D	80 (64%)	3 (30%)	1 (20%)	0 (0%)	7 (24%)	3 (38%)	5 (83%)	7 (100%)	9 (90%)	45 (98%)
	I	78 (62%)	1 (10%)	1 (20%)	0 (0%)	10 (36%)	2 (25%)	5 (83%)	7 (100%)	8 (80%)	44 (96%)
Bone Matrix	O	68 (54%)	0 (0%)	0 (0%)	0 (0%)	2 (7%)	2 (25%)	4 (67%)	5 (71%)	9 (90%)	46 (100%)
	D	71 (57%)	3 (30%)	0 (0%)	0 (0%)	2 (7%)	2 (25%)	4 (67%)	6 (86%)	9 (90%)	45 (98%)
	I	67 (54%)	1 (10%)	0 (0%)	0 (0%)	2 (7%)	1 (13%)	5 (83%)	6 (86%)	8 (80%)	44 (96%)
Bone Resorption	O	14 (11%)	0 (0%)	0 (0%)	0 (0%)	2 (7%)	3 (38%)	1 (17%)	3 (43%)	0 (0%)	5 (11%)
	D	24 (19%)	0 (0%)	0 (0%)	0 (0%)	3 (10%)	3 (38%)	1 (17%)	4 (57%)	2 (20%)	11 (24%)
	I	17 (14%)	0 (0%)	0 (0%)	0 (0%)	3 (11%)	2 (25%)	0 (0%)	4 (57%)	2 (20%)	6 (13%)
Woven Bone	O	10 (8%)	0 (0%)	0 (0%)	0 (0%)	1 (3%)	0 (0%)	1 (17%)	1 (14%)	2 (20%)	5 (11%)
	D	17 (14%)	0 (0%)	0 (0%)	0 (0%)	0 (0%)	0 (0%)	2 (33%)	3 (43%)	3 (30%)	9 (20%)
	I	15 (12%)	0 (0%)	0 (0%)	0 (0%)	0 (0%)	0 (0%)	3 (50%)	3 (43%)	1 (10%)	8 (17%)
Lamellar Bone	O	65 (52%)	0 (0%)	0 (0%)	0 (0%)	2 (7%)	2 (25%)	2 (33%)	5 (71%)	8 (80%)	46 (100%)
	D	67 (54%)	2 (20%)	0 (0%)	0 (0%)	1 (3%)	2 (25%)	3 (50%)	6 (86%)	8 (80%)	45 (98%)
	I	62 (50%)	1 (10%)	0 (0%)	0 (0%)	1 (4%)	0 (0%)	3 (50%)	6 (86%)	7 (70%)	44 (96%)
Reversal Lines	O	62 (50%)	0 (0%)	0 (0%)	0 (0%)	3 (10%)	3 (38%)	4 (67%)	6 (86%)	5 (50%)	41 (89%)
	D	58 (46%)	0 (0%)	0 (0%)	0 (0%)	3 (10%)	2 (25%)	4 (67%)	6 (86%)	5 (50%)	38 (83%)
	I	60 (48%)	1 (10%)	0 (0%)	0 (0%)	5 (18%)	2 (25%)	4 (67%)	6 (86%)	4 (40%)	38 (83%)

Color code:

	>0-25%
	26-50%
	51-75%
	75-100%

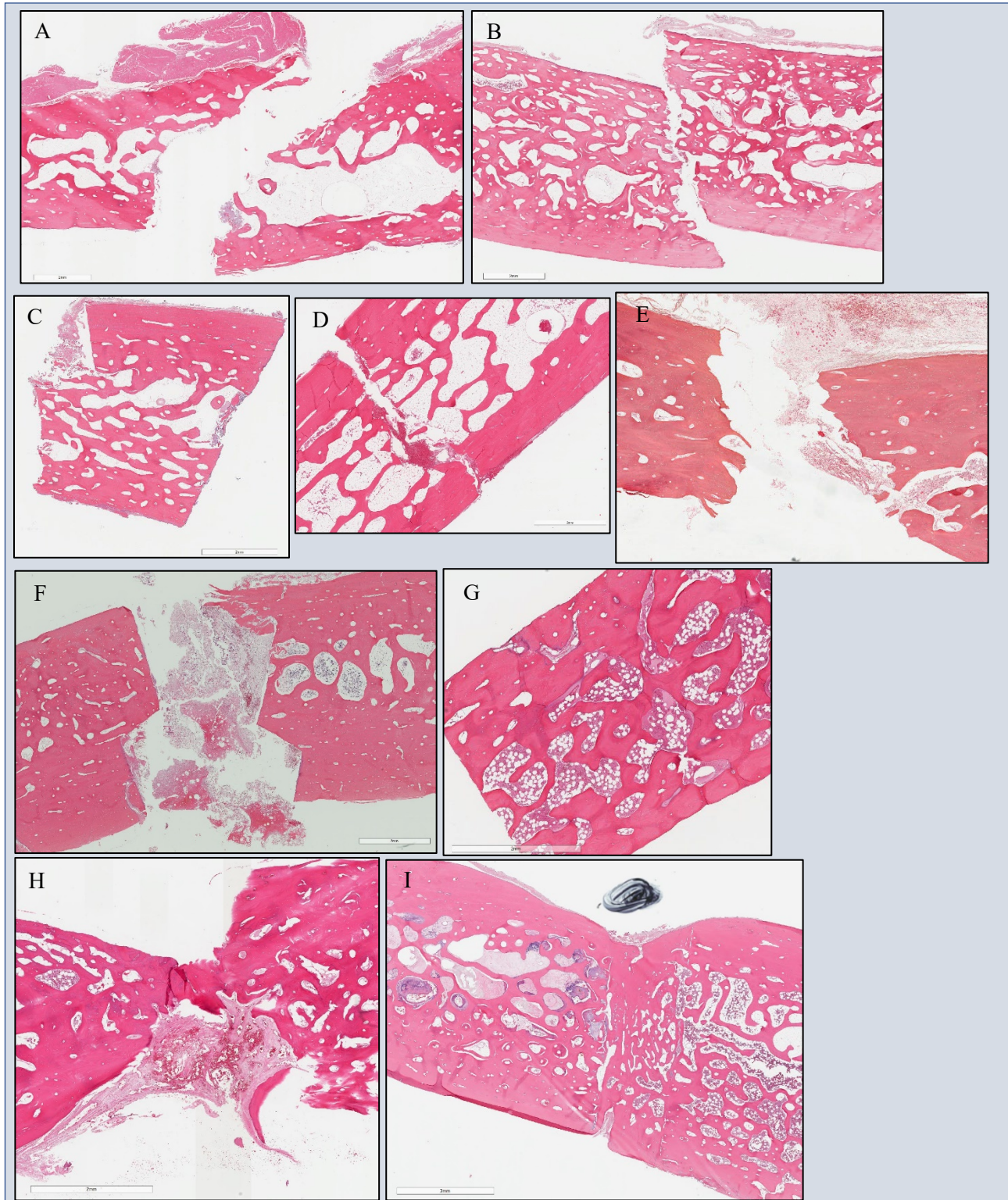


Figure 11. Histological slide photomicrographs of injuries to the cranial vault at varying times of healing. (A) Acute, (B) 1 hour, (C) 14 hours, (D) 2 days 12 hours, (E) 12 days 20 hours, (F) 22 days, (G) 4 months, (H) 1 year 4 months, (I) 10 years.

Table 17. Adult extent scores. Color coding is based on the maximum mean extent.

Feature	Zone	Acute	0-1 hr	1-24 hr	1-7 d	7-14 d	14-30 d	1-6 mo	6-18 mo	18+ mo
TOTAL		10	5	4	29	8	6	7	10	46
Hematoma Organization Extent (1-4)	O	5 (0.08 - 0.58)	1 (1.08 - 1.08)	1 (0.08 - 0.08)	24 (0.33 - 2.17)	5 (0.50 - 1.50)	5 (0.17 - 2.00)	3 (0.17 - 2.08)	3 (0.42 - 1.08)	8 (0.33 - 1.33)
	D	7 (0.08 - 0.67)	1 (0.42 - 0.42)	1 (0.08 - 0.08)	25 (0.08 - 2.83)	5 (0.33 - 1.42)	5 (0.42 - 1.83)	3 (0.50 - 2.42)	3 (0.67 - 1.75)	7 (0.33 - 1.33)
	I	4 (0.17 - 0.92)	1 (1.00 - 1.00)	1 (0.25 - 0.25)	23 (0.08 - 2.17)	5 (0.08 - 1.00)	5 (0.17 - 2.00)	4 (0.33 - 2.67)	3 (0.67 - 1.75)	11 (0.25 - 1.33)
Fibrin Extent (1-4)	O	3 (0.67 - 0.67)	1 (0.33 - 0.33)	1 (0.25 - 0.25)	25 (0.33 - 2.00)	4 (0.33 - 1.33)	3 (0.33 - 2.33)	1 (1.67 - 1.67)	2 (0.67 - 2.00)	7 (0.33 - 1.00)
	D	5 (0.67 - 1.33)	1 (0.33 - 0.33)	1 (0.25 - 0.25)	25 (0.33 - 3.33)	5 (0.33 - 1.33)	5 (0.67 - 2.67)	1 (2.67 - 2.67)	4 (0.67 - 2.00)	6 (0.33 - 0.67)
	I	4 (0.33 - 1.00)	1 (1.00 - 1.00)	1 (0.25 - 0.25)	24 (0.33 - 2.67)	4 (0.67 - 1.33)	3 (1.67 - 2.00)	2 (0.33 - 2.33)	3 (0.67 - 2.00)	6 (0.33 - 1.00)
Fracture Edge (1=Sharp 2=Blurred 3=n/a)	O	10 (1.00 - 1.67)	5 (1.00 - 2.33)	4 (1.00 - 2.83)	29 (1.00 - 2.33)	8 (1.00 - 1.67)	6 (1.33 - 2.00)	7 (1.33 - 2.17)	10 (1.33 - 2.67)	46 (1.67 - 3.00)
	D	10 (1.00 - 1.67)	5 (1.00 - 1.33)	4 (1.00 - 1.33)	29 (1.00 - 1.67)	8 (1.00 - 1.67)	6 (1.33 - 2.00)	7 (1.33 - 2.42)	10 (1.25 - 2.67)	46 (1.67 - 3.00)
	I	10 (1.00 - 1.67)	5 (1.00 - 1.33)	4 (1.00 - 1.33)	28 (1.00 - 1.67)	8 (1.00 - 1.67)	6 (1.33 - 2.00)	7 (1.33 - 2.08)	10 (1.08 - 2.67)	46 (1.67 - 3.00)
Fibroblasts/cytes Frequency (1-4)	O	4 (0.08 - 0.50)	2 (0.42 - 0.58)	1 (0.08 - 0.08)	18 (0.08 - 1.83)	5 (1.42 - 2.00)	5 (0.17 - 2.08)	6 (0.33 - 3.08)	7 (0.17 - 1.08)	39 (0.08 - 3.00)
	D	3 (0.08 - 1.92)	1 (0.17 - 0.17)	1 (0.08 - 0.08)	14 (0.08 - 2.92)	5 (1.00 - 2.00)	5 (1.17 - 2.08)	7 (0.17 - 3.25)	7 (0.08 - 2.33)	37 (0.25 - 3.00)
	I	2 (0.08 - 0.25)	2 (0.08 - 0.17)	1 (0.25 - 0.25)	10 (0.08 - 2.00)	5 (0.17 - 1.25)	5 (0.25 - 1.58)	6 (0.33 - 2.83)	4 (0.25 - 1.92)	39 (0.08 - 3.00)
Fibrous CT/collagen Extent (1-4)	O	4 (0.33 - 1.00)	1 (1.50 - 1.50)	2 (0.67 - 0.67)	16 (0.17 - 2.83)	6 (0.67 - 2.17)	4 (0.67 - 2.67)	6 (0.17 - 3.00)	6 (0.33 - 1.33)	40 (0.33 - 4.00)
	D	2 (0.67 - 1.67)	1 (1.50 - 1.50)	1 (0.67 - 0.67)	11 (0.17 - 2.00)	6 (0.17 - 2.33)	5 (0.67 - 3.00)	7 (0.17 - 3.33)	7 (0.33 - 2.83)	37 (0.17 - 4.00)
	I	3 (0.17 - 0.67)	2 (0.33 - 1.00)	1 (1.00 - 1.00)	11 (0.17 - 2.00)	4 (0.33 - 1.00)	4 (0.67 - 2.17)	5 (0.50 - 2.83)	7 (0.17 - 2.67)	41 (0.33 - 3.83)
New Capillaries Extent (1-4)	O	2 (0.58 - 0.67)	1 (0.42 - 0.42)	1 (0.33 - 0.33)	13 (0.08 - 1.42)	5 (0.50 - 1.58)	4 (0.50 - 2.75)	4 (0.67 - 2.42)	7 (0.17 - 1.33)	33 (0.08 - 2.92)
	D	2 (0.75 - 1.08)	1 (0.42 - 0.42)	1 (0.33 - 0.33)	9 (0.08 - 1.50)	6 (0.25 - 1.58)	5 (0.83 - 2.67)	6 (0.33 - 2.42)	7 (0.42 - 2.58)	38 (0.08 - 3.33)
	I	1 (0.08 - 0.08)	2 (0.08 - 0.67)	1 (0.67 - 0.67)	8 (0.08 - 1.67)	5 (0.08 - 1.33)	5 (0.25 - 2.08)	5 (0.08 - 2.50)	5 (0.08 - 1.83)	35 (0.08 - 3.00)
Lamellar Bone Extent (1-4)	O	6 (0.33 - 0.58)	3 (0.58 - 1.33)	1 (0.08 - 0.08)	16 (0.17 - 2.25)	4 (0.33 - 1.33)	4 (0.58 - 1.67)	7 (0.33 - 3.33)	10 (0.58 - 3.33)	46 (1.33 - 4.00)
	D	7 (0.25 - 0.75)	3 (0.33 - 1.00)	1 (0.17 - 0.17)	16 (0.17 - 2.00)	4 (0.33 - 1.75)	4 (0.33 - 1.58)	6 (0.92 - 3.33)	10 (0.58 - 3.50)	46 (0.92 - 4.00)
	I	6 (0.33 - 1.17)	3 (0.50 - 1.00)	1 (0.67 - 0.67)	15 (0.17 - 2.08)	5 (0.17 - 0.67)	4 (0.67 - 1.58)	7 (0.17 - 3.25)	10 (0.42 - 3.33)	46 (0.42 - 4.00)

Color code:

>0-1	Minimal
>1-2	Mild
>2-3	Moderate
>3-4	Extensive

To better distinguish the reparative process, the extents of the following features were investigated to derive their nuanced changes over time: hematoma organization, fibrin, fracture edge blurring, fibroblasts, fibrous connective tissue/collagen, new capillaries, and lamellar bone.

Adult extent scores are summarized in Table 17. The first value in each cell represents the number of samples for which the feature was scored as present in any evaluation for that anatomical zone, followed by the range of the mean extent values across all samples. The color coding is based upon the maximum mean extent. This table shows that when hematoma peaks in the 1-7 day range, that it reaches a moderate extent of expression. When fibrin peaks during the 1-7 day period, its expression varies by zone from mild to extensive. With fracture edge, it is evident that by 18+ months there are many fractures that are scored as N/A or 3 which indicates the fracture edge is unobservable because bone has completely healed across the fracture gap. Fibroblasts/cytes reached the greatest extent in samples that were between 1 and 6 months old but remained at a moderate extent for injuries that were more than 18 months old. New capillaries peak at 14-30 days and beyond and during these time periods their extent is mild to extensive, varying by age and anatomic zone. Finally, lamellar bone has extensive representation in samples 1-6 months and older.

A summary of the analysis of covariation of assessed features is presented in Table 18 (full covariation results in Table 24 in the Appendix). This table shows that hematoma, organization, and fibrin presence are all highly correlated. Pigment laden macrophages have high covariation with both cartilage and inflammation, but this is because these features were rarely seen in the sample. All of the sub-features under the connective tissue category (mesenchyme/loose connective tissue, fibroblasts/cytes, fibrous connective tissue/collagen) all have the highest covariance with connective tissue. Capillaries also show the highest covariance with connective tissue. The sub-features of the bone formation/remodeling category, including bone matrix, bone resorption, woven bone, lamellar bone, and reversal/cement lines, all show

their highest covariance with other features within this category. Blurring of fracture edge also has a high co-occurrence with lamellar bone presence.

Table 18. Summary of the highest covariations of features without regard to healing time

FEATURE	HIGHEST COVARIATION	RANGE	MEAN
Hematoma*	Fibrin*	0.91 to 0.99	0.96
Organization*	Fibrin	0.89 to 0.99	0.95
Pigment*	Cartilage*	0.94 to 0.97	0.96
Inflammation*	Pigment	0.92 to 0.94	0.93
Connective Tissue*	Fibrous CT/Collagen*	0.92 to 1.0	0.96
Mesenchyme/Loose CT*	Connective Tissue	0.77 to 0.98	0.89
Fibroblasts/cytes*	Connective Tissue	0.91 to 1.0	0.96
Capillaries*	Connective Tissue	0.91 to 1.0	0.95
Fracture Edge*	Lamellar Bone	0.96 to 0.98	0.97
Bone Formation*	Bone Matrix	0.96 to 1.0	0.99
Bone Matrix*	Lamellar Bone*	0.99 to 1.0	1.0
Bone Resorption*	Bone Formation	0.57 to 0.95	0.83
Woven Bone*	Bone Matrix	0.73 to 0.94	0.87
Reversal/Cement Lines*	Bone Formation	0.94 to 0.99	0.97

* indicates it was also the highest covariation for listed feature.

Infant and Juvenile Healing

The sample sizes for the infants and juveniles are too small for statistical analysis, however each of these individuals represents an important contribution to understanding cranial fracture repair. As such, each case will be discussed from the acute injury state to more advanced healing. The presence of tissues and cells involved in infant and juvenile healing was drawn from the majority agreement of two evaluators. These values are included in Tables 22 and 23 in the Appendix. Tables 19 and 20 include the mean extents of all three evaluators using all stains. Since the tissue extents are documented as ordinal variables between 0 (absent) and 4 (extensive), a mean extent of less than 1 indicates that only one of three evaluators documented

the presence and extent of the tissue. Therefore, any score less than 1 is excluded from the assessment. The following descriptions include all three zones, unless otherwise specified.

Description of Infant Samples

FH-065 and FH-012 are infants with acute linear fractures and serve as controls representing fractures with no healing. Although one evaluator noted the minimal presence of healing tissues, reevaluation by the PIs found no evident healing response.

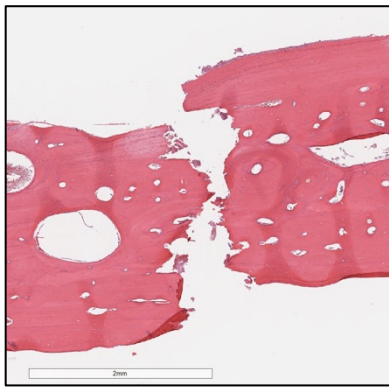


Figure 12. Photomicrograph of FH-012 acute fracture sample

FH-001 is an infant with two areas of circular injuries to the left and right parietals. These are birth injuries attributed to vacuum assisted delivery with an injury age of 20 days. Tissues and extents include a mild to moderately organized hematoma, minimal to mild fibrin in the outer and inner zones, acute to chronic inflammation with mild intensity and focal to patchy distribution, minimal to mild mesenchyme, rare to mild fibroblasts/cytes, mild to moderate fibrous connective tissue, minimal to mild new capillaries, and minimal cartilage matrix. The osseous response is exhibited by a blurred fracture margin, a reversal line in the diploic zone, and minimal woven bone in the outer and inner zones.

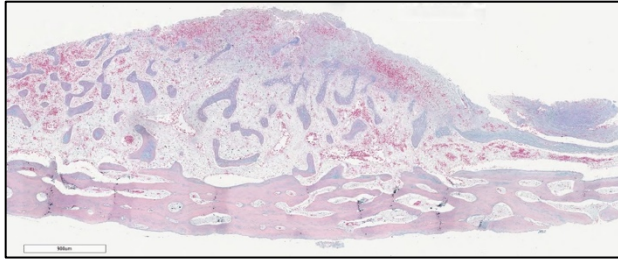


Figure 13. FH-001 photomicrograph of parietal injury aged 20 days

There are three infants (FH-002, FH-053, and FH-089) in the study with an unknown age of injury, however it is assumed the injuries are not older than the decedents' age. Although they were primarily included for the inter-observer agreement portion of the study, each will be described.

FH-002 has multiple healing linear cranial fractures with investigative evidence suggesting the injuries were inflicted on multiple occasions. Three samples were taken at postmortem examination of fractures that grossly appeared to be at three different stages of healing. For ease of comparison, the samples are described from minimal to extensive healing. Sample 2 is composed of minimal to mild mesenchyme in the diploic and inner zones, mild to moderate fibroblasts/cytes, minimal to mild fibrous connective tissue, and the osseous response includes a blurred fracture margin, and a reversal line in the outer and inner zones. Sample 1 is composed of minimal to mild fibrin in the outer and inner zones, minimal to moderate mesenchyme, mild to moderate fibroblasts/cytes, minimal to mild fibrous connective tissue, minimal new capillaries, minimal to mild woven bone, a blurred fracture margin, and a reversal line in the outer zone. Sample 3 is composed of minimal hematoma organization in the outer and inner zones, minimal to moderate mesenchyme, mild to moderate fibroblasts/cytes, mild to moderate fibrous connective tissue, minimal to mild new capillaries, minimal to moderate

cartilage, a blurred fracture margin, minimal to mild woven bone, minimal lamellar bone in the diploic zone, and a reversal line.

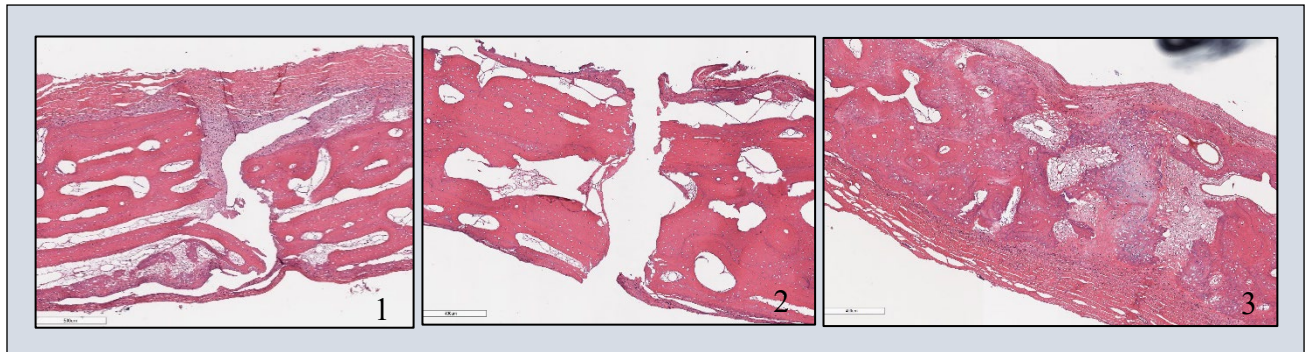


Figure 14. Three fracture samples aged 1-3 months from case FH-002

FH-053 is an infant represented by six samples from a single linear fracture on the left parietal. The samples vary slightly, primarily in the presence or absence of an inflammatory response. Tissue presence and extents include minimal to mild hematoma organization, minimal fibrin, inflammation (present in 2 samples), minimal to mild mesenchyme, moderate to extensive fibroblasts/cytes, moderate to extensive fibrous connective tissue, mild to moderate new capillaries, bone resorption, mild to moderate woven bone, minimal to mild lamellar bone, a blurred fracture margin, and reversal line.

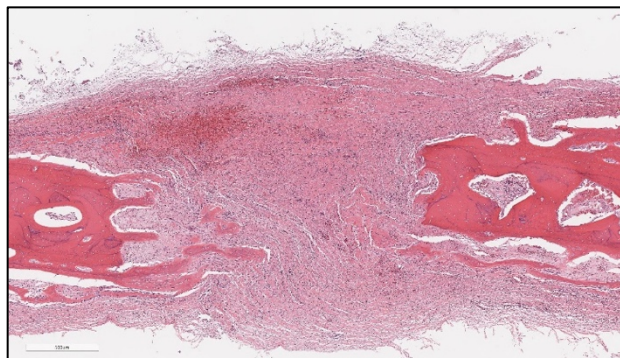


Figure 15. FH-053 healing fracture

FH-089 is an infant for which three samples from multiple linear fractures of the right parietal and occipital were submitted with little variation in the constitution of each. The samples are composed of minimal to mild hematoma organization (Sample 3 only), minimal fibrin (Sample 3 only), minimal mesenchyme (Sample 3 only), mild to moderate fibroblasts/cytes, moderate to extensive fibrous connective tissue, minimal to moderate new capillaries, minimal cartilage, mild to moderate woven bone, minimal to mild lamellar bone, a blurred fracture margin, and a reversal line.

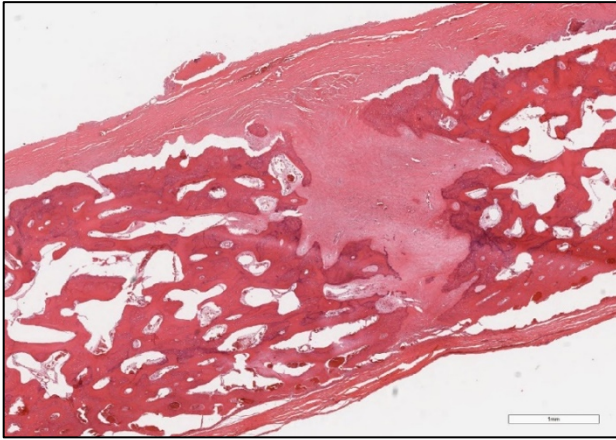


Figure 16. FH-089 healing fracture

Table 19. Extent averages for infant samples

Sample:		FH-065-S1	FH-012-S1	FH-053-S1a	FH-053-S1b	FH-053-S1c	FH-053-S1d	FH-053-S1e	FH-053-S1f	FH-001-S1	FH-002-S1	FH-002-S2	FH-002-S3	FH-089-S1	FH-089-S2	FH-089-S3
Injury Type:		Linear	Linear	Linear	Linear	Linear	Linear	Linear	Linear	Other	Linear	Linear	Linear	Linear	Linear	Linear
Healing Time:		0 days	0 days	8-28 days	8-28 days	8-28 days	8-28 days	8-28 days	8-28 days	20 days	1-3 months	1-3 months	1-3 months	3-8 months	3-8 months	3-8 months
FEATURE	ZONE															
Organization Extent (1-4)	Outer	0	0.25	1.33	0.92	1.5	1	2.67	2	2.67	0	0	1	0	0	1.33
	Diploë	0	0.42	1.33	1.08	1.17	0.75	1.33	0.75	1.25	0	0	0	0	0	1.33
	Inner	0	0	1.33	1	1	0.75	1.33	1.17	1.08	0	0	1	0	0	0
Fibrin Extent (1-4)	Outer	0	0.33	0	1	0.33	0.67	0	0	1.33	0	0	0	0	0	1
	Diploë	0	0.67	0	1	0	0.33	0	0	0.67	0	0	0	0	0	1
	Inner	0	0	0	1	0	0.33	0	0	1.67	0	0	0	0	0	0
Inflammation Type (1=Acute, 2=Chronic, 3=Mixed)	Outer	0	0	0.83	1.25	0	0.5	0.67	0.17	2.08	0.17	0	0	0	0	0.67
	Diploë	0	0	0.83	1.25	0	0	0.67	0	1.67	0.17	0	0	0	0	0.67
	Inner	0	0	0.83	1.25	0	0.17	0.67	0	1.58	0	0	0	0	0	0
Inflammation Intensity (1=Mild, 2=Moderate, 3=Severe)	Outer	0	0	0.75	0.83	0	0.25	0.42	0.08	1.25	0.08	0	0	0	0	0.33
	Diploë	0	0	0.75	0.75	0	0	0.42	0	0.75	0.08	0	0	0	0	0.33
	Inner	0	0	0.75	0.75	0	0.08	0.33	0	0.67	0	0	0	0	0	0
Inflammation Distribution (1=Focal, 2=Patchy, 3=Widespread)	Outer	0	0	1.08	1.25	0	0.5	0.92	0.17	1.83	0.08	0	0	0	0	0.33
	Diploë	0	0	1.08	1.25	0	0	1	0	1.33	0.08	0	0	0	0	0.33
	Inner	0	0	1.08	1.25	0	0.17	1	0	1.17	0	0	0	0	0	0
Fracture Edge (1=Sharp, 2=Blurred, 3=n/a)	Outer	1.17	1.17	2	2	2	2	2	2	1.92	1.67	1.33	2	2	2	2
	Diploë	1.08	1	2	2.08	2	2	2	2	1.75	1.83	1.33	2	2	2	2
	Inner	1.17	1.25	2	2	2	1.92	2	2	1.75	1.67	1.33	2	2	2	2
Mesenchyme Extent (1-4)	Outer	0.33	0	0	0	0.5	0.58	1.17	0.58	1.75	1.92	0.58	0.83	0.33	0.17	1.17
	Diploë	0	0	0	0	0.67	0.42	1.5	0.67	1.42	2.42	1.42	3	0.25	0.25	1.25
	Inner	0.08	0	0	0	0.42	0.58	1.17	0.67	1	1.25	1.42	1	0.42	0.25	1.33
	Outer	0.25	0.75	3.67	3.67	3.58	3.33	3	3.08	2.17	2.58	2.92	2.83	2.17	2.5	2.67

Fibroblast/cyte Frequency (1-4)	Diploë	0	0	3.75	3.67	3.67	3.33	3	2.83	1.58	2.42	1.83	2.5	2.42	2.67	2.67
	Inner	0.17	0	3.67	3.67	3.33	3.25	3	2.67	1.5	2.17	2.17	2.58	2.25	2.5	2.58
Fibrous CT/collagen Extent (1-4)	Outer	0.67	0.67	3.67	3.67	3.67	3.83	3.33	4	2.67	2.17	2.33	2.5	3	3.5	3.67
	Diploë	0	0	3.83	3.83	3.67	4	3.33	4	2	1.5	1.67	2.17	3	3.83	3.67
	Inner	0.17	0	3.67	3.67	3.67	3.67	3.67	3.83	1.67	1.83	1.83	2.33	3.33	3.67	3.67
New Capillaries Extent (1-4)	Outer	0.42	0	3.17	2.67	2.58	2.42	2.08	2.17	2.08	1.25	0.17	1.17	1.92	1.92	2.25
	Diploë	0	0	3.17	2.42	2.67	2.58	2.33	2.25	1.83	1	0.67	2.17	2.92	2.25	2.33
	Inner	0.08	0	3	2.08	2.83	2.25	2.25	2.25	1.25	0.83	0.75	1.17	2.5	1.67	2.17
Cartilage Matrix Extent (1-4)	Outer	0	0	0.56	0	0	0	0.22	0.11	0.89	0.22	0	1.11	0.78	0.89	0.89
	Diploë	0	0	0.22	0	0	0	0.22	0.22	0.67	0	0.33	3	1	0.89	1
	Inner	0	0	0	0	0	0	0.33	0.11	0.89	0.11	0.44	1.22	1.22	1	0.89
Woven Bone Extent (1-4)	Outer	0	0	2.83	2.58	2.25	1.92	2	1.58	0.58	1.17	0.67	0.75	3.08	3.08	2
	Diploë	0	0	2.92	2.5	2.5	2	2	1.67	0.33	0.75	0.42	2.17	3.33	3.08	2.42
	Inner	0	0	2.83	2.5	2.92	2.08	2.58	1.58	0.75	1.33	0.75	0.83	3.25	3	2.25
Lamellar Bone Extent (1-4)	Outer	0.33	0.42	1.75	1.67	0.42	1.83	1.25	1.33	0	0.67	0.33	0.33	1.75	1.92	1.17
	Diploë	0.08	0.33	1.92	1.83	0.5	1.58	1.08	1.33	0	0.25	0.75	1	1.83	2	1.25
	Inner	0.17	0.25	1.75	1.58	1.08	2.33	1.33	1.42	0	0.33	0.42	0.67	1.75	1.83	1.33

Color code:

	>0-1	Minimal
	>1-2	Mild
	>2-3	Moderate
	>3-4	Extensive

Description of Juvenile Samples

The juvenile sample includes individuals ranging from 3 years to 15 years of age with linear cranial fractures. The cases are presented from the most acute injury to most advanced healing (Table 19).

FH-014 is a decedent with a sub-acute fracture to the left parietal (1 hour). Although some tissues were noted by one evaluator, no healing response is evident.

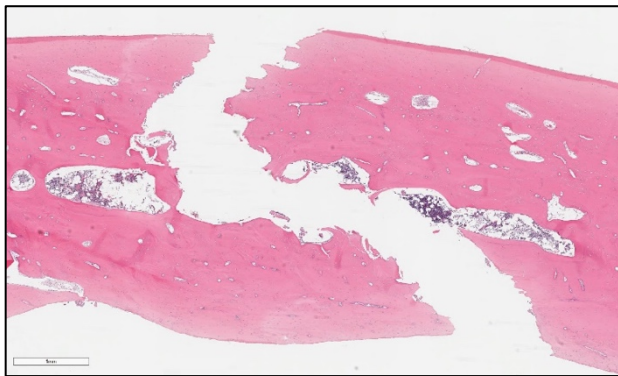


Figure 17. FH-014 parietal fracture healed 1 hour

FH-008 is a decedent with multiple linear fractures. Three samples were collected for this individual; one (Sample 4) from the bone flap that was removed three hours after the injury and two samples (Sample 1 and 2) from the vault representing 3 days of healing. Although some tissues were noted in Sample 4 by one evaluator, no healing response is evident. Sample 1 is a linear fracture from the occipital with a healing time of three days. This sample is composed of minimal to mild mesenchyme, mild to moderate fibroblasts/cytes in the outer and diploic zones, minimal to mild fibrous connective tissue in the outer and diploic zones, minimal to mild new capillaries in the outer and diploic zones, minimal to mild cartilage in the diploic zone, a blurred fracture margin, and a reversal line in the diploic zone. Sample 2 is a linear fracture from the left parietal with a healing time of three days. The sample is composed of mild hematoma

organization, minimal fibrin in the inner zone, moderate fibrin in the diploic zone, an inflammatory response, blurred fracture margin, and reversal line.

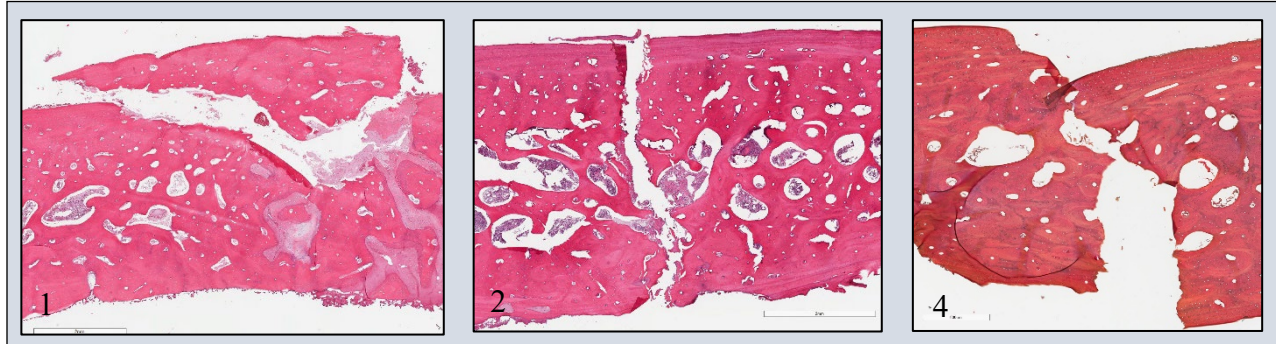


Figure 18. FH-008 fracture samples: (1) linear fracture healed 3 days, (2) linear fracture healed 3 days, (4) linear fracture on bone flap with 3.5 hours of healing

FH-041 is a decedent with a linear fracture of the frontal with a healing time of almost 13 days. The fracture is composed of minimal hematoma organization in the diploic and inner zones, minimal to mild fibrin, an inflammatory response, mild to moderate mesenchyme, mild to moderate fibroblasts/cytes, minimal to moderate fibrous connective tissue, minimal to mild new capillaries, minimal to mild cartilage in the outer and diploic zones, minimal to mild woven and lamellar bone, a reversal line, and blurred fracture margin.

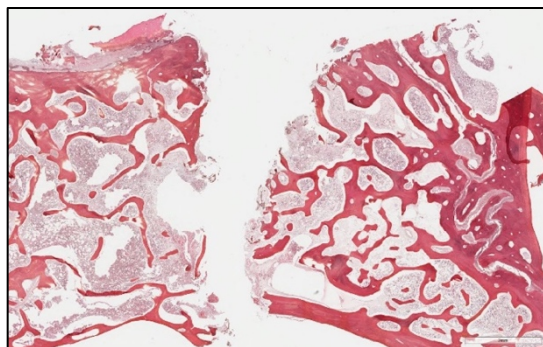


Figure 19. FH-041 healing linear fracture aged 12 days and 20 hours

FH-028 is a decedent with two healed linear fractures of the left parietal with an injury age of approximately 9 years. Sample 1 is a healed fracture with a complete bone bridge. It is

composed of minimal mesenchyme, moderate lamellar bone, and a complete bone bridge. FH-028 Sample 2 is a healed linear fracture with a bone bridge spanning the outer zone. It is composed of rare fibroblast/cytes in the diploic and inner zones, minimal to mild fibrous connective tissue, minimal new capillaries in the diploic zone, minimal lamellar bone, reversal lines, and a blurred fracture margin in the diploic and inner zones.

Table 20. Extent averages for juvenile samples

Sample:		FH-014-S2	FH-008-S4	FH-008-S1	FH-008-S2	FH-041-S1	FH-028-S1	FH-028-S2
Injury Type:		Linear	Linear	Depressed	Linear	Linear	Linear	Linear
Healing Time:		1 hour	3.5 hours	3 days	3 days	12 days, 20 hours	9 years, 3 months	9 years, 3 months
FEATURE	ZONE							
Organization Extent (1-4)	Outer	0	0	0.08	0	0.42	0	0
	Diploë	0	0	0.17	2.25	0.75	0.58	0.58
	Inner	0	0	0	0.67	0.83	0	0.17
Fibrin Extent (1-4)	Outer	0	0	0	0	1	0	0
	Diploë	0	0	0	2.67	1.33	0.67	0
	Inner	0	0	0	1.33	1.67	0	0
Inflammation Type (1=Acute, 2=Chronic, 3=Mixed)	Outer	0	0	0	0	0.92	0	0.17
	Diploë	0.75	0	0	2.33	2.42	0	1
	Inner	0	0	0	0.08	0.83	0	0.25
Inflammation Intensity (1=Mild, 2=Moderate, 3=Severe)	Outer	0	0	0	0	0.42	0	0.08
	Diploë	0.33	0	0	1.08	0.92	0	0.42
	Inner	0	0	0	0.08	0.33	0	0.08
Inflammation Distribution (1=Focal, 2=Patchy, 3=Widespread)	Outer	0	0	0	0	0.5	0	0.17
	Diploë	0.42	0	0	1.58	1.5	0	0.42
	Inner	0	0	0	0.08	0.58	0	0.08
Fracture Edge (1=Sharp, 2=Blurred, 3=n/a)	Outer	1.08	1.08	1.33	1.25	2	3	2.58
	Diploë	1.08	1.08	1.33	1.33	2	2.67	1.92
	Inner	1.08	1.08	1.33	1.33	1.92	2.83	1.92
Mesenchyme Extent (1-4)	Outer	0.25	0.08	2.17	0	2	0	0.5
	Diploë	0.25	0.08	1.33	0.42	2.08	0.92	0.58
	Inner	0.08	0	0	0	1.83	0	0.25
Fibroblasts/cytes Frequency (1-4)	Outer	0.17	0.08	2.08	0.58	2.5	0	0.92
	Diploë	0.17	0	2.42	1.17	2.17	0.67	0.92
	Inner	0.08	0	0	0.5	1.42	0.33	0.67
Fibrous CT/collagen Extent (1-4)	Outer	0	0	2	0.83	2.67	0	1.67
	Diploë	0	0	2	0.83	2.33	0.5	1.67
	Inner	0	0	0.33	0.5	1	0.5	1.67
New Capillaries Extent (1-4)	Outer	0	0	1.5	0	1.33	0	0.33
	Diploë	0	0	1.5	0.33	1.75	0.67	0.83
	Inner	0	0	0	0	1.08	0.17	0.33
Cartilage Matrix Extent (1-4)	Outer	0	0	0	0.22	1.56	0	0
	Diploë	0	0	1.44	0	1.44	0	0.44
	Inner	0	0	0	0	0.22	0.11	0.11
Woven Bone Extent (1-4)	Outer	0	0	0	0	1.67	0	0
	Diploë	0	0	0	0.08	1.25	0.33	0
	Inner	0	0	0	0	0.42	0.08	0
Lamellar Bone Extent (1-4)	Outer	0	0.5	0.67	0.25	1.92	2.75	1.42
	Diploë	0.5	0.5	0.75	0.17	1.75	2.58	1.17
	Inner	0.17	0.5	0.67	0.25	1	2.67	1.08

Color code:

	>0-1	Minimal
	>1-2	Mild
	>2-3	Moderate
	>3-4	Extensive

Stages of Healing in the Adult Cranial Vault

This study shows that there is a marked difference between cranial and postcranial healing in the adult. First, there is no external callus stage. In typical postcranial fracture healing, there is a tandem process of intramembranous and endochondral ossification, however the degree of weight bearing and biomechanical factors can influence whether there is fibrous connective tissue or cartilage involved at the healing site⁸. We see an almost complete absence of cartilage development in cranial bone healing. A likely explanation for this is the minimal strain, stress, hydrostatic pressure, and movement on the cranial vault since there is little to no muscle action or weight bearing. This environment would likely result in decreased signaling for chondroblastic activity effectively eliminating a cartilaginous soft callus⁸.

Hematoma

The initial response to a cranial fracture or defect is a hematoma. A hematoma may be observed immediately after injury, but it is more likely to be seen in the 1-7 day range when it is organized with moderate amounts of fibrin. These features then wane and resolve after 14-30 days. While it may be surprising that hematoma is not more prevalent in the 0-1 hour and 1-24 hour range, this may be due to the fact that it is not yet organized and thus is more likely to be lost during sample removal, fixation, or decalcification. Although inflammatory cells are rarely seen, they are most likely to be observed in the 1-7 day range, disappearing thereafter.

Soft Tissue Response

As fracture repair is a continuous process, it is expected there will be overlap between stages of healing. As the initial responses of hematoma and inflammation are peaking in the 1-7 day period, this is also the time period when reparative processes begin. Connective tissue components, including mesenchyme/loose connective tissue, fibroblasts/cytes, and collagen/fibrous connective tissue, appear in the 1-7 day range, peak in the 14-30 day range and typically resolve after 1-6 months. Although there are relatively few observations of connective tissue features in the 6-18 month period, there is another peak in the 18+ months category. This peculiar phenomenon in the 18+ months bin is likely capturing injuries that were bridged with fibrous connective tissue rather than bone, an expected outcome in defects with wide fracture gaps. In concert with fibrous connective tissue infiltration, the formation of new capillaries is also observed starting between 1 and 7 days, peaking between 14 and 30 days and declining thereafter. The higher prevalence in the 18+ months category is likely a reflection of normal remodeling processes.

Osseous Repair

The osseous response to injury in our sample generally begins in the 1-7 day range and continues until the bone is healed. There are a couple of examples of osseous response prior to this time period, but they represent injuries sustained in unwitnessed motor vehicle accidents, so the exact time of death is unknown. The majority of samples show evidence of osseous activity in the 14-30 day period with evidence of bone matrix, reversal lines and blurred fracture margins. By the 30-180 day (1-6 months) time period and beyond, nearly every sample has evidence of osseous activity, the most prevalent being bone matrix, lamellar bone, and reversal lines. These features continue to have a high prevalence for the remainder of the injury age

categories (6-18 months, and 18+ months). Although osseous activity is common in advanced healing, evidence for bone resorption and woven bone are relatively rare within the sample. Bone resorption peaks in the 1-6 month range with 43-57% of samples showing evidence, but outside this time period it is not regularly observed. Woven bone is even less common with its highest prevalence between the 14-30 day (17-50%) and 30-180 day (14-43%) ranges.

Discussion

This study highlights the differences between cranial and postcranial bone repair in adults. Postcranial bone repair is typically divided into four stages: inflammation, soft callus, hard callus, and remodeling. The first difference is evident with the initial response to bone injury, as our sample shows little evidence of an inflammatory response. Cranial vault repair also lacks both the soft callus and hard callus stages that are common in postcranial repair, with a virtual absence of both cartilage and woven bone. Rather, the fracture gap is filled initially with connective tissue and then lamellar bone is laid down perpendicular to the fractured cortical bone. This type of repair is known as “gap healing,” a type of direct fracture healing that occurs if there are stable conditions and a relatively small fracture gap⁹. However, if the fracture gap is wide, fibrous connective tissue may persist indefinitely. Without a soft and hard callus, the traditional remodeling phase is also lacking in cranial defect repair. In fact, most of the injuries in the 18+ month range are still visible without complete remodeling and reestablishment of diploe, although our sample may be biased towards cranial injuries that are still grossly evident years later.

Another surprising outcome of this study is a notable lack of osteoclasts and evidence of osteoclastic activity (Howship’s lacunae) despite the blurring of fracture margins. This remodeling along the fracture edge may be due to the presence of lysosomal cell lines which

degrade margins via acid hydrolases and promote apoptosis in the cells along the fracture margins¹⁰.

While the sample sizes for infants and juveniles are too small for analysis, there are some interesting observations that seem to distinguish the cranial healing process in these younger ages. While inflammation and cartilage are still rare in these groups, 11 of the 15 infant samples (73.3%) have woven bone present in at least one of the anatomic zones, and 9 (60.0%) of the samples have it in all three zones. In juveniles, however, only 1 sample has evidence of woven bone.

There were notable outcomes from this study that were not part of the research design. Evaluators were asked to evaluate several soft and hard tissue responses to injury, however they were not asked to evaluate how and in what orientation new bone is formed in the fracture gap. In general, woven bone is rare (especially in adults) and new bone formation is composed of lamellar bone. Whether the injury is due to surgical intervention or linear fracture, this new lamellar bone is deposited appositionally along each side of the fracture gap and is oriented perpendicular to the parent bone matrix. This orientation can still be seen years after the injury.

Conclusion

The Repository of Antemortem Injury Response (REPAIR) serves as an invaluable tool for the forensic community as the first database to bring together comprehensive recorded and visual data of cranial injuries of known ages. Through the compilation of this dataset under a secure yet easily accessible digital interface, the limitations imposed upon cranial fracture studies, such as difficulties in obtaining a robust sample, are mitigated. Researchers wishing to use the data housed in REPAIR may visit the site and register themselves and their prospective purpose in using information from the database. Upon approval of the proposed study by the platform

administrators, the requested data can be exported from REPAIR via a *csv* file and provided to the interested party. Visual data, such as photographs, radiographs, and scanned photomicrographs are also available to the research community. Additionally, the repository was designed in a manner such that postcranial fractures of known ages could be submitted and stored in the future with only minor adjustments, thus broadening the scope and utility of the data housed within REPAIR. The database is also useful for comparative assessments of cranial fracture and medical interventions in forensic casework. On the broader scope of influence, it serves the forensic community as a means to increase communication and collaboration between institutions through the continued addition of known age injuries to its population.

Beyond the value of REPAIR, this is the first study to document the histological progression and develop unique stages of osseous healing for the human cranial vault. The stages of cranial fracture repair and associated histological features at different injury ages developed herein give investigators a preliminary tool to assess the age of cranial fractures, eliminating any prior reliance on postcranial models of healing and subjective estimations dependent upon analyst experience. Discernment of the histological trajectory of healing in the cranial vault and its characterization through stages shall act as the foundation of the authors' continued research to develop a comprehensive time since injury estimation method. Outside the scope of forensic science, the clarity afforded to the scientific community via this groundbreaking model of cranial fracture repair will inherently be of use to tissue engineering and other researchers interested in augmenting rates of healing in the human cranium.

An important contribution of this project was the development of a method to assess healing injuries of the vault. One of the deficiencies in forensic science has been the lack of understanding of how cranial vault bones heal. This deficiency is largely due to the absence of

appropriate histological training. Forensic anthropologists and forensic pathologists are minimally trained in normal and abnormal decalcified bone histology. Forensic anthropology training focuses on dry bone or ground bone histology and forensic pathologists focus on soft tissue morphology. As such, much time was spent with the evaluators to familiarize them with the presentation of the cells and tissues in healing bone.

This experience has led the investigators to plan for a future workshop at the American Academy of Forensic Sciences annual meeting. This workshop will serve to train forensic pathologists and anthropologists in fracture healing histology and the value of using this information to inform future interpretations of cranial trauma for time-since injury. In addition, the profession of forensic anthropology is currently focused on standardizing education at the post graduate level. The educational materials and didactics from this workshop will constitute the basis for a fracture healing manual to incorporate into the graduate curriculum.

The experimental sub-studies assessing histological staining and decalcification will allow histological technicians and investigators, interested in assessing healing in human bone, an empirical basis for selecting a decalcification agent and/or histological stain. Better informed methodologies will help to streamline the development of histological slides for research and forensic casework by reducing time investments, improving assessment accuracy, and preventing unnecessary destruction of osseous samples.

Limitations

A power analysis performed during the design phase of the study showed a sample size of 84 was required to achieve a medium (0.3) significant correlation effect between histological elements and time since injury. To account for specimens which were not suitable for testing, a

target sample goal was set at 100 samples for each of the three age cohorts: infants (0 to 36 months), juveniles (36 months to 16 years), and adults (16+ years), resulting in a total of 300 cases of known age cranial fractures. To achieve this sample size, partnerships were established, and material transfer agreements were executed with medical examiner offices across the country. Unfortunately, only samples from 3 decedents were obtained from partnering institutions. While the goal was still able to be met for the adult cohort, the infant and juvenile cohorts consist of 15 and 7 samples, respectively. Interestingly, many of the subadult samples that were contributed to the study had diastatic fractures rather than linear fractures (and were subsequently excluded from further analysis), demonstrating the ability of the immature cranium to dissipate energy through the sutures rather than fracturing. Thus, the evaluation of histological features of healing in concert with progressing time in the antemortem interval could only be done for the adult age group. While some understanding of the tissue and cellular responses to cranial fractures in infants and juveniles could be ascertained, the progressions could not be linked with time due to the small working samples. The results of the adult healing phases presented herein should not be applied to calvarial fractures in individuals younger than 16 years. It was observed in numerous studies that the rate of fracture healing in children, especially those under the age of two, is greatly increased in comparison to adults¹¹⁻¹⁴. Furthermore, the structure of the cranial vault bone shifts from unilaminar to diploic beginning in the 4th year of life, potentially impacting the process of fracture repair¹⁵. Through the continued growth of REPAIR, the authors hope to derive the stages of healing and their associated time since injury for infants and juveniles at a future time. For now, the model of cranial vault healing developed through this research should be applied only upon the population of age 16 years and above.

Although our adult sample was robust, once it was divided into different age categories it was apparent that some injury age groups were underrepresented. This limited our ability to conduct robust statistical analyses comparing these different injury age groups. Furthermore, it was impossible in the development of the sample to control all factors which may alter the rate of fracture/injury repair in the cranial vault. Aspects of decedent history and injury such as the fracture severity, bone type, surgical interventions, patient ancestry, drug use, and co-morbidities may alter the rate and histological process of healing in the cranial vault. As the sample population of REPAIR becomes more robust, assessments to elucidate the influence of these confounding variables upon fracture healing in the cranium can be undertaken. This would allow for the development of tailored methods for aging fractures in individuals of varying demographics, medical histories. and injury circumstances.

Collaborating Institutions

The primary source of cranial vault fractures for building the REPAIR database came from medical examiner (ME) cases at this study's host research institution, Western Michigan University Homer Stryker M.D. School of Medicine (WMed) Forensic and Autopsy Service. Additional samples were sourced through WMED's body donation program and the following partner institutions:

- Macomb County Medical Examiner's Office, Mt. Clemens, Michigan
- Pima County Office of the Medical Examiner, Tuscon, Arizona

The number of cases contributed by each institution to the REPAIR database is listed in Table 18. The contributing offices were notified of the opportunity to submit samples to the database through the National Association of Medical Examiners listserv. Each partnering medical examiner office was required to complete a material transfer agreement developed by

the project PIs prior to sending fracture samples to WMed. Training in sample procurement methods was disseminated to the sampling partners, and shipping kits for sample transfers were assembled at the host institution and sent to the ME offices as needed.

Table 21. REPAIR sample contributions by institution

Institution	Samples Contributed
Western Michigan University Homer Stryker M.D. School of Medicine Forensic and Autopsy Service	144
WMed Body Donation Program	1
Macomb County Medical Examiner’s Office	6
Pima County Office of the Medical Examiner	4

Scholarly Products Produced/In Progress

Publications

Submitted

Isaac CV, Cornelison JB, Prahlow JA, Devota CJ, Christensen E. *An Overview of Fracture Healing and the Repository of Antemortem Injury Response (REPAIR): An Online Database for Skeletal Injuries of Known Ages*. Manuscript submitted for publication.

In Preparation

A manuscript of the results of the decalcification agent time and quality assessment is in draft and will be submitted for publication in Summer 2021.

A manuscript of the results of the histological stain assessment for fracture histomorphology is in draft and will be submitted for publication in Summer 2021.

A publication of the observed histological stages of cranial fracture repair for adult individuals aged 16+ years in a condensed form across each of the three anatomical zones is planned.

Conference Presentations

2020

Cornelison JB, Isaac CV, Lackey-Cornelison W, Shattuck B, deJong JL, Fisher-Hubbard AO, Brown TT, Douglas EA, Prahlow JA. (2020). The Histomorphology of Cranial Fracture Healing: Preliminary Observations. Presented at the 72nd annual meeting of the American Academy of Forensic Sciences in Anaheim, CA.

Isaac CV, Cornelison JB, Prahlow JA. (2020). The Repository of Antemortem Injury Response (REPAIR): An Invaluable Online Resource of Known Age Fractures for Comparison and Research. Presented at the 72nd annual meeting of the American Academy of Forensic Sciences in Anaheim, CA.

Isaac CV, Cornelison JB, Prahlow JA. (2020). The Repository of Antemortem Injury Response (REPAIR): An Invaluable Online Resource of Known Age Fractures for Comparison and Research. Presented on February 7 at Michigan State University Anthropology Department's 5th Annual Graduate Student Research Symposium, East Lansing, MI.

2019

Isaac CV, Cornelison JB, Christensen ER. (2019). The Repository of Antemortem Injury Response (REPAIR): An Online Reference of Known Time Since Fractures. Presented at the 9th annual meeting of the Forest, Lakes, and Grasslands (FLAG) Forensic Anthropologists, Roscommon, MI.

Isaac CV, Cornelison JB, Prahlow JA. (2019). The Histomorphology of Cranial Fracture Healing: Case Examples. Poster presented at the 71st annual meeting of the American Academy of Forensic Sciences in Baltimore, MD.

Cornelison JB, Isaac CV, Prahlow JA. (2019). A Comparison of Three Methods for Assessment of Bone Decalcification Time and Quality of Histological Slides for Cranial Fracture Healing Investigation. Poster presented at the 71st annual meeting of the American Academy of Forensic Sciences in Baltimore, MD.

2018

Cornelison JB, Isaac CV, Prahlow JA. (2018). Preliminary Observations for the Histology of Fracture Healing. Presented at the 8th annual meeting of the Forest, Lakes, and Grasslands (FLAG) Forensic Anthropologists, Roscommon, MI.

2017

Cornelison JB, Isaac CV (2017). Histological Investigation of Healing Cranial Trauma. Presented at the Seventh Annual Forests, Lakes, and Grasslands Regional Conference, Roscommon, MI, October 2016.

Database

The Repository of Antemortem Injury Response (REPAIR)

REPAIR (repair.orainc.com), developed in collaboration with ORA, is a burgeoning database housing known-age cranial fracture cases with comprehensive written, radiographic, photographic and photomicrograph sample documentation for use in research and comparative casework assessments.

Training

A sample procurement module for training purposes was developed and disseminated to partnering Medical Examiner Offices to ensure standard sample collection. The module describes the required radiography, gross examination photography, and sampling and storage guidelines for shipping.

A training module was prepared for the evaluators to introduce the four different histological stains and the histology sample evaluative form.

Acknowledgements

The project's Principal Investigators would like to acknowledge Jon Langworthy and Kristi Bailey of the Research Histology Laboratory at Western Michigan University Homer Stryker M.D. School of Medicine (WMED) for their phenomenal contributions in developing histological slides for this project. A tremendous thank you to Joeseeph Billian, M.S., of WMED's Department of Epidemiology and Biostatistics for his design and execution of the statistical elements of this study. To the project's histological evaluators, Theodore Brown, M.D., Joyce deJong, D.O., Elizabeth Douglas, M.D., Amanda Fisher-Hubbard, M.D., Wendy Lackey-Cornelison, Ph.D., and Brandy Shattuck, M.D., we are forever grateful for your immense efforts which have propelled the next components of this project forward. To the Chief Medical Examiner and Chair of the Department of Pathology at WMED, Dr. Joyce deJong, D.O., thank you for your endless support, encouragement, and stalwart leadership which has paved the way for the success of this project. Finally, we would like to thank Erica Christensen, M.S., and Kerianne Armelli, M.S., for their support in populating the REPAIR database.

Bibliography

1. Sfeir C, Bab IA. Bone Regeneration and Repair. Totowa, NJ: Humana Press, 2005.
2. Prosser I, Maguire S, Harrison SK, Mann M, Sibert JR, Kemp AM. How Old Is This Fracture? Radiologic Dating of Fractures in Children: A Systematic Review. *Am J Roentgenol* 2005;184(4):1282–6. <https://doi.org/10.2214/ajr.184.4.01841282>.
3. Prosser I, Lawson Z, Evans A, Harrison S, Morris S, Maguire S, et al. A Timetable for the Radiologic Features of Fracture Healing in Young Children. *Am J Roentgenol* 2012;198(5):1014–20. <https://doi.org/10.2214/AJR.11.6734>.
4. Maat GJR. Case Study 5.3: Dating of Fractures in Human Dry Bone Tissue - the Berisha Case. In: Kimmerle EH, Baraybar JP, editors. *Skeletal Trauma*. Boca Raton, Florida: Taylor & Francis Group, 2008;245–54.
5. Boyd DC. The anatomical basis for fracture repair. *Forensic Anthropology*. Chichester, UK: John Wiley & Sons, Ltd, 2018;149–200.
6. Augat P, Simon U, Liedert A, Claes L. Mechanics and mechano-biology of fracture healing in normal and osteoporotic bone. *Osteoporos Int* 2005;16(S02):S36–43. <https://doi.org/10.1007/s00198-004-1728-9>.
7. Marston L. *Introductory Statistics for Health and Nursing Using SPSS*. 1 Oliver’s Yard, 55 City Road, London EC1Y 1SP United Kingdom: SAGE Publications Ltd, 2010.
8. Claes L., Heigele C. Magnitudes of local stress and strain along bony surfaces predict the course and type of fracture healing. *J Biomech* 1999;32(3):255–66. [https://doi.org/10.1016/S0021-9290\(98\)00153-5](https://doi.org/10.1016/S0021-9290(98)00153-5).

9. Marsell R, Einhorn TA. The biology of fracture healing. *Injury* 2011;42(6):551–5.
<https://doi.org/10.1016/j.injury.2011.03.031>.
10. Guicciardi ME, Leist M, Gores GJ. Lysosomes in cell death. *Oncogene* 2004;23(16):2881–90. <https://doi.org/10.1038/sj.onc.1207512>.
11. Gaston MS, Simpson AHRW. Inhibition of fracture healing. *J Bone Joint Surg Br* 2007;89-B(12):1553–60. <https://doi.org/10.1302/0301-620X.89B12.19671>.
12. Glaser MA, Blaine ES. Fate of Cranial Defects Secondary to Fracture and Surgery. *Radiology* 1940;34(6):671–84. <https://doi.org/10.1148/34.6.671>.
13. Mirhadi S, Ashwood N, Karagkevrekis B. Factors influencing fracture healing. *Trauma* 2013;15(2):140–55. <https://doi.org/10.1177/1460408613486571>.
14. Wraight PJ, Scammell BE. Principles of fracture healing. *Surg* 2006;24(6):198–207.
<https://doi.org/10.1383/surg.2006.24.6.198>.
15. Koenig WJ, Donovan JM, Pensler J. Cranial Bone Grafting in Children. *Plast Reconstr Surg* 1995;95(1):1–4.

Appendix

LIST OF TABLES

TABLE 22. HISTOLOGICAL FEATURE PRESENCE/ABSENCE FOR INFANT SAMPLES	62
TABLE 23. HISTOLOGICAL FEATURE PRESENCE/ABSENCE FOR JUVENILE SAMPLES	64
TABLE 24. COVARIATION OF FEATURE PRESENCE IN ALL ADULT FRACTURES	66

Table 22. Histological feature presence/absence for infant samples

	Sample:	FH-065-S1	FH-012-S1	FH-053-S1a	FH-053-S1b	FH-053-S1c	FH-053-S1d	FH-053-S1e	FH-053-S1f	FH-001-S1	FH-002-S1	FH-002-S2	FH-002-S3	FH-089-S1	FH-089-S2	FH-089-S3
	Injury Type:	Linear	Linear	Linear	Linear	Linear	Linear	Linear	Linear	Other	Linear	Linear	Linear	Linear	Linear	Linear
	Fracture Healing Time:	0 days	0 days	8-28 days	8-28 days	8-28 days	8-28 days	8-28 days	8-28 days	20 days	1-3 months	1-3 months	1-3 months	3-8 months	3-8 months	3-8 months
FEATURE	ZONE															
Hematoma	Outer				X	X	X	X	X	X						
	Diploë		X		X	X	X			X						
	Inner				X	X	X			X						
Organization	Outer					X		X	X	X						
	Diploë									X						
	Inner									X						
Pigment	Outer															
	Diploë															
	Inner															
Fibrin	Outer									X						
	Diploë		X							X						
	Inner									X						
Inflammation	Outer				X					X						
	Diploë				X					X						
	Inner				X					X						
Fracture Edge Blurred	Outer			X	X	X	X	X	X	X	X		X	X	X	X
	Diploë			X	X	X	X	X	X	X	X		X	X	X	X
	Inner			X	X	X	X	X	X	X	X		X	X	X	X
Connective Tissue	Outer			X	X	X	X	X	X	X	X	X	X	X	X	X
	Diploë			X	X	X	X	X	X	X	X	X	X	X	X	X
	Inner			X	X	X	X	X	X	X	X	X	X	X	X	X
Mesenchyme	Outer							X		X	X					X
	Diploë							X		X	X	X	X			X

	Inner							X		X	X	X				X
Fibroblasts	Outer			X	X	X	X	X	X	X	X	X	X	X	X	X
	Diploë			X	X	X	X	X	X	X	X	X	X	X	X	X
	Inner			X	X	X	X	X	X	X	X	X	X	X	X	X
Collagen	Outer			X	X	X	X	X	X	X	X	X	X	X	X	X
	Diploë			X	X	X	X	X	X	X	X	X	X	X	X	X
	Inner			X	X	X	X	X	X	X	X	X	X	X	X	X
Capillaries	Outer			X	X	X	X	X	X	X	X		X	X	X	X
	Diploë			X	X	X	X	X	X	X	X		X	X	X	X
	Inner			X	X	X	X	X	X	X	X		X	X	X	X
Cartilage Formation	Outer									X			X		X	
	Diploë												X		X	
	Inner									X			X		X	
Bone Formation	Outer			X	X	X	X	X	X		X	X	X	X	X	X
	Diploë			X	X	X	X	X	X		X	X	X	X	X	X
	Inner			X	X	X	X	X	X	X	X	X	X	X	X	X
Bone Matrix	Outer			X	X	X	X	X	X		X	X	X	X	X	X
	Diploë			X	X	X	X	X	X		X	X	X	X	X	X
	Inner			X	X	X	X	X	X	X	X	X	X	X	X	X
Bone Resorption	Outer			X	X	X	X	X	X					X	X	X
	Diploë			X	X	X	X	X	X					X	X	X
	Inner			X	X	X	X	X	X					X	X	X
Woven Bone	Outer			X	X	X	X	X	X		X			X	X	X
	Diploë			X	X	X	X	X	X				X	X	X	X
	Inner			X	X	X	X	X	X		X			X	X	X
Lamellar	Outer			X	X		X	X	X					X	X	X
	Diploë			X	X		X	X	X					X	X	X
	Inner			X	X	X	X	X	X					X	X	X
Reversal	Outer			X	X	X	X	X	X		X	X		X	X	X
	Diploë			X	X	X	X	X	X	X			X	X	X	X
	Inner			X	X	X	X	X	X			X	X	X	X	X

Table 23. Histological feature presence/absence for juvenile samples

	Sample:	FH-014-S2	FH-008-S4	FH-008-S1	FH-008-S2	FH-041-S1	FH-028-S1	FH-028-S2
	Injury Type:	Linear	Linear	Depressed	Linear	Linear	Linear	Linear
	Healing Time:	1 hour	3.5 hours	3 days	3 days	12 days, 20 hours	9 years, 3 months	9 years, 3 months
FEATURE	ZONE							
Hematoma	Outer							
	Diploë				X	X		
	Inner				X			
Organization	Outer							
	Diploë				X	X		
	Inner				X			
Pigment	Outer							
	Diploë							
	Inner							
Fibrin	Outer							
	Diploë				X	X		
	Inner				X	X		
Inflammation	Outer							
	Diploë				X	X		
	Inner							
Fracture Edge Blurred	Outer					X	.	X
	Diploë					X	X	X
	Inner			X		X	.	X
Connective Tissue	Outer			X		X		X
	Diploë			X	X	X		X
	Inner			X		X		X
Mesenchyme	Outer			X		X		
	Diploë			X		X		X
	Inner					X		
Fibroblasts	Outer			X		X		X
	Diploë			X	X	X		X
	Inner					X		
Collagen	Outer			X		X		X
	Diploë			X	X	X		X
	Inner			X		X		X
Capillaries	Outer			X		X		
	Diploë			X		X		X
	Inner					X		
Cartilage Formation	Outer					X		
	Diploë			X		X		
	Inner							
Bone Formation	Outer					X	X	X
	Diploë					X	X	X
	Inner			X		X	X	X
Bone Matrix	Outer					X	X	

This resource was prepared by the author(s) using Federal funds provided by the U.S. Department of Justice. Opinions or points of view expressed are those of the author(s) and do not necessarily reflect the official position or policies of the U.S. Department of Justice.

	Diploë					X	X	X
	Inner			X		X	X	X
Bone Resorption	Outer					X		
	Diploë					X		
	Inner					X		
Woven Bone	Outer					X		
	Diploë					X		
	Inner							
Lamellar	Outer					X	X	X
	Diploë					X	X	X
	Inner			X		X	X	X
Reversal	Outer					X		X
	Diploë				X	X	X	X
	Inner			X		X	X	X

